Post-fire behaviour of ferritic stainless steel material

Elsevier Editorial System(tm) for
Construction & Building Materials
Manuscript Draft

Manuscript Number: CONBUILDMAT-D-17-02904R1

Title: Post-fire Behaviour of Ferritic Stainless Steel Material

Article Type: Research Paper

Keywords: Cooling rate; ferritic stainless steel; mechanical properties; microstructure; post-fire; stress-strain curve.

Corresponding Author: Dr. Yuner Huang, PhD

Corresponding Author's Institution: The University of Edinburgh

First Author: Yuner Huang, PhD

Order of Authors: Yuner Huang, PhD; Ben Young, PhD

Abstract: Ferritic stainless steel have a high potential to be used as structural material, as it has a desirable mechanical properties and a relatively low price compared with other stainless steel materials. However, the post-fire mechanical properties of ferritic stainless steel have not been investigated up to now. This paper presents an experimental investigation on mechanical properties of ferritic stainless steel after exposed to high temperatures up to 1000°C. Residual mechanical properties and microstructure of the specimens are examined. The ferritic stainless steel specimens were cooled down by four different cooling methods, namely cool-in-chamber, cool-in-air, cool-in-air-with-fan and cool-in-water. It is shown that different cooling rates have minor effects on the strengths of ferritic stainless steel, but it affects the strain and Ramberg-Osgood parameter (n) in a certain temperature range. It is shown that the current design rules cannot provide accurate predictions for the post-fire mechanical properties of ferritic stainless steel materials. Therefore, a unified design equation is proposed to predict the post-fire mechanical properties, and a stress-strain model is also proposed to predict the post-fire stress-strain relationship when the specimens are cooled down in chamber from 24 to 1000 °C. Reliability analysis has also conducted to assess the reliability of the proposed design rules. It is shown that the modified stress-strain models compare well with the experimental results throughout the full range of stress-strain curves.

SCHOOL *of* ENGINEERING

Dr Yuner Huang
INSTITUTE *for* INFRASTRUCTURE *and* ENVIRONMENT
The University of Edinburgh
William Rankine Building
Thomas Bayes Road
Edinburgh EH9 3FG
Scotland, UK
Tel: +44 (0)131 650 5736
Email: yuner.huang@ed.ac.uk

07 September 2017

Dear Professor Crews,

I wish to submit a revised paper entitled "Post-fire Behaviour of Ferritic Stainless Steel Material" to be considered for publication in *Journal of Construction and Building Materials*. All the reviewers' comments have been considered and addressed.

This paper presents a comprehensive experimental and theoretical study on ferritic stainless steel material after exposed to high temperatures. Ferritic stainless steel is a relatively new material to be used as structural elements in construction industry. But it has gained increasing attention in the construction industry, as it has a high strength-to-cost ratio compared with other stainless steel material, and excellent fire resistant properties compared with carbon steel. The investigation on their post-fire mechanical properties provides evidence in repair and reinforcement of stainless steel structures after fire hazards, and thus reduce economic losses of fire and improve sustainability of the built environment. We believe that this manuscript is appropriate for publication by *Journal of Construction and Building Materials*, because it match with the scope of the journal, such as repair and maintenance of high-rise buildings, civil engineering structures, housing. I believe it will be of great interest of the readers of *Journal of Construction and Building Materials*.

I have no conflicts of interest to disclose. Please address all correspondence concerning this manuscript to me at Yuner.huang@ed.ac.uk.

Thank you for your consideration of this manuscript.

Sincerely,

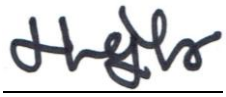

Yuner Huang

Written explanation and changes (CONBUILDMAT-D-17-02904)

Journal: Construction & Building Materials

Title of Paper: Post-fire Behaviour of Ferritic Stainless Steel Material

Authors: Yuner Huang and Ben Young

Ms. Ref. No.: CONBUILDMAT-D-17-02904

The authors appreciate the reviewers for their useful comments. The reviewers' comments have been seriously considered and addressed accordingly below:

Reviewer #1

Comment 1: The paper presents an experimental study of the post-fire material properties of ferritic stainless steels. The experimental procedures, obtained results and discussions on findings are presented. The paper provides useful data on post-fire properties of ferritic stainless steels.

Authors' reply: Thank you very much for the positive comments.

Comment 2: However, some general issues related to the use of ferritic stainless steels in construction remain unanswered. Are ferritic stainless steels used/will be used in structural applications where fire is potentially a hazard? Can examples of such applications perhaps be given in the introduction part of the paper?

Authors' reply: The authors agree with the reviewer's comment. The following sentences describing structural applications of ferritic stainless steel, where fire is potentially a hazard, has been added in Section 1. Two additional references are added.

"Ferritic stainless steel has been applied as construction material in buildings, houses, roofing of large-span structures and bridges in Europe, Japan and South Africa [1]. Fire is a potential hazard in these applications. Further structural applications of ferritic stainless steels have been investigated in a Research Fund for Coal and Steel (RFCS) project of "Structural Applications of Ferritic Stainless Steels (SAFSS)" [2], which develops design guidelines and technical information sheet for engineers and architects to use ferritic stainless steel in structural components."

Comment 3: How are the findings of this research, in a broader context, used to ensure safety of these structures following a post-fire event?

Authors' reply: The research outcome can be used to predict residual Young's modulus and strength of the material after the structures exposed to elevated temperatures. This information can be used to estimate the structural integrity after fire hazards. As mentioned by the Reviewer #3, the relevant results and analytical models can be referred to in the fire engineering design of stainless steel structure. A sentence "*The relevant results and analytical models can be referred to in the fire engineering design of stainless steel structure*" is added at the end of the first paragraph.

Reviewer #3

Comment 1: This paper presents an experimental investigation into the post-fire behaviour of ferritic stainless steel materials. The relevant results and analytical models can be referred to in the fire engineering design of stainless steel structure.

Authors' reply: Thank you very much for the positive comments.

Comment 2: However, this paper was less logically presented with some English grammar errors included in some sentences. The discussion of the test results was less critical and less in depth. Hence, it is anticipated that this paper could be considered for the publication in the Journal of Construction and Building Materials, if the authors could thoroughly review the paper and address the following additional issues satisfactorily.

Authors' reply: The authors agree with the reviewer's comment. The paper has been reviewed carefully, and all the issues pointed out by the reviewer have been addressed accordingly.

Comment 3: Page 2, Paragraph 2, line 2, the word of "researches"?

Authors' reply: A typo error has been corrected. The word of "researches" is replaced by "researchers".

Comment 4: Between those in Page 2, lines 9 to 14 and Page 3, line 1 to 3, there seem some kind of similarity and repletion.

Authors' reply: The authors agree with the reviewer's comment. The sentences have been rewritten to avoid similarity and repletion.

Comment 5: Page 3, Paragraph 2, lines 3 to 4, an improvement for grammar of the sentence.

Authors' reply: The authors agree with the reviewer's comment. The revised sentence with an improvement for grammar is as followed:
"In recent years, some researches were conducted to improve the Ramberg-osgood model, where 2-stage models were used for a more accurate prediction."

Comment 6: Page 3, Paragraph 3, lines 3 to 6 might need to follow the description of testing methods in lines 7 to 10.

Authors' reply: The authors agree with the reviewer's comment. Rearrange of sentences has been made accordingly.

Comment 7: Page 4, Paragraph 2. It seems both steel type and specimen dimensions have less explicitly defined. To what extend do the different sizes of RHS sections affect the type of a stainless steel? In addition, explain the reason why a reference was made to AS1979 and ASTM2002, but not to Eurocodes.

Authors' reply:
- In this study, the same steel type (EN 1.4003 or ASTM S40977) is used for all test specimens of different RHS sections. Therefore, the different sections do not affect the type of stainless steel.
- The steel type of the specimen has been added in the paragraph.
- The coupon dimension agrees with the requirement in Eurocode. The European Code (BS EN ISO 6892-2: 2011) has been added in the paragraph and reference list.

Comment 8: Page 5, paragraphs 1 and 2, it seems unusual to start from Fig.2 before Fig. 1 in description of your test procedure.

Authors' reply: The authors agree with the reviewer's comment. The figures have been rearranged. The text in this paragraph has also been updated accordingly.

Comment 9: Pages 5 and 6, please explain the reason why two different oven/furnace were used in your tests. To what extend can the results of the specimens that were

heated /cooled in different oven/furnace be comparable?

Authors' reply: Two different oven/furnace were used to investigate a comprehensive post-fire mechanical properties. Firstly, the MTS high temperature furnace is specially designed to allow for strain measurement of test specimen under elevated temperatures. Therefore, thermal expansion (Table 1 and Fig. 20) can be accurately measured with the furnace, and such measurement is not possible with the oven. Secondly, the heating elements in MTS furnace are easily broken under rapid cooling from high temperature. The furnace can only be used to investigate the cool-in-chamber case, but not the other cooling processes. Therefore, Catterson Smith annealing oven was used to investigate post-fire mechanical properties under cool-in-air, cool-in-air-with-fan and cool-in-water cases. Third, thermal couples were attached at each specimen to monitor the actual specimen temperature during heating and cooling process in the two different furnace/oven. The measured specimen temperature of each specimen during soak time was used in analysis. Therefore, the use of two different furnace/oven has minimum impact to the research outcome.

Comment 10: Page 5, last two lines. It seems that the different cooling methods were only applied after 500C. Compared with 1000oC, is it significant? To what extend your results and conclusions about the effect of cooling rate can be referred by practical engineer?

Authors' reply:

- Test results for F1 and F2 specimens have shown that the stress-strain behaviour of ferritic stainless steel generally remain the same when the exposed temperature is lower than 500°C (Table 1). Similar conclusion can be drawn from literatures for other steel materials (Fig.8 – Fig.10). Therefore, different cooling methods were only applied after 500°C.
- The test results shown that the different cooling methods have negligible effects for Young's modulus, yield strength and ultimate strength of ferritic stainless steel specimens after being exposed to elevated temperatures ranging from 600 to 1000 °C. The following sentence is added, so that the work can be referred by practical engineer.
  "…, thus it does not affect the repair and reinforcement scheme of stainless steel structures after fire hazards."

Comment 11: Page 6, lines 12 to 18, it seems too much repetition about the cooling rates/methods.

Authors' reply: The authors agree with the reviewer's comment. The paragraph has been re-written to reduce repetition.

Comment 12: Page 6, paragraph 2, it seems unusual to use the displacement control before the yielding of a steel specimen. Explain its potential effect on the measured properties of steel specimens.

Authors' reply: The European Code (BS EN ISO 6892-1) allows strain rate control for coupon tests before the yielding of a steel specimen, which recommends a maximum strain rate of 15×10^{-3} (min^{-1}). The strain rate measured during the coupon tests is smaller than 15×10^{-3} (min^{-1}), thus it agrees with the European Code.

Comment 13: Page 7, line 8, Table 3(?)

Authors' reply: It should be Table 2, instead of Table 3. This typo error has been corrected.

Comment 14: Figs 6 and 8 to 13 were reasonably well presented, but less critically and precisely discussed in pages 8 to 9. For example, the variation of ultimate strength in Fig 10 is actually not the same as those of hardness in Fig 6. If the results in Fig 13 are for the specimen with the soak time of 20 minutes, what about those in Figs 8 to 13. The mechanism of variations in these Figs was less significantly explored.

Authors' reply: The authors agree with the reviewer's comment. The paragraphs in page 8-9 has been revised for a more precise discussion.

Comment 15: Page 9, paragraph 3, lines 4 to 8, less precise description with some grammar error included.

Authors' reply: The authors agree with the reviewer's comment. The paragraph has been re-written. Grammatical errors have been corrected.

Comment 16: Page 11, Paragraph 2, last two lines, the description seems not fully consistent with those shown in Figure 20.

Authors' reply: The authors agree with the reviewer's comment. Figure 20 has shown the comparison between test and design values, and thus the last sentence has been deleted to avoid confusion.

Comment 17: Page 12, Paragraphs 2, line 8. No comparison can be found in Figs 13, 15, 16, and 17.

Authors' reply: The authors agree with the reviewer's comment. The comparison between test results and design values calculated by proposed equation is not shown in Figs 13-17. Therefore, the paragraph has been revised that only Figs 8-12 is mentioned.

Comment 18: Page 15, re-write the section of the conclusion and make it more precisely and specifically

Authors' reply: The authors agree with the reviewer's comment. The conclusion has been re-written.

Highlights

- Investigation on ferritic stainless steel post-fire mechanical properties was performed.
- Effects of exposed temperature, soak time and cooling rate are investigated.
- The exposed temperatures ranged from 24 to 1000 ºC.
- Existing design rules are assessed by comparing test results.
- Design rules to predict residual mechanical properties were proposed.
- Constitutive model to predict stress-strain curves after fire exposure was proposed.

Post-fire Behaviour of Ferritic Stainless Steel Material

Yuner Huang[1*], and Ben Young[2]

[1]* Lecturer, School of Engineering, The University of Edinburgh, Mayfield Road, Edinburgh, United Kingdom.

Email: yuner.huang@ed.ac.uk

[2] Professor, Department of Civil Engineering, The University of Hong Kong, Pokfulam Road, Hong Kong.

ABSTRACT

Ferritic stainless steel have a high potential to be used as structural material, as it has a desirable mechanical properties and a relatively low price compared with other stainless steel materials. However, the post-fire mechanical properties of ferritic stainless steel have not been investigated up to now. This paper presents an experimental investigation on mechanical properties of ferritic stainless steel after exposed to high temperatures up to 1000°C. Residual mechanical properties and microstructure of the specimens are examined. The ferritic stainless steel specimens were cooled down by four different cooling methods, namely cool-in-chamber, cool-in-air, cool-in-air-with-fan and cool-in-water. It is shown that different cooling rates have minor effects on the strengths of ferritic stainless steel, but it affects the strain and Ramberg-Osgood parameter (n) in a certain temperature range. It is shown that the current design rules cannot provide accurate predictions for the post-fire mechanical properties of ferritic stainless steel materials. Therefore, a unified design equation is proposed to predict the post-fire mechanical properties, and a stress-strain model is also proposed to predict the post-fire stress-strain relationship when the specimens are cooled down in chamber from 24 to 1000 °C. Reliability analysis has also conducted to assess the reliability of the proposed design rules. It is shown that the modified stress-strain models compare well with the experimental results throughout the full range of stress-strain curves.

KEYWORDS: Cooling rate; ferritic stainless steel; mechanical properties; microstructure; post-fire; stress-strain curve.

1. INTRODUCTION

Stainless steel has a high corrosion resistance compared with carbon steel. It has been increasingly used in recent years as a structural material especially in medium-to-high corrosion applications, due to its aesthetic appearance and ease in future maintenance as well as a longer life cycle. Ferritic stainless steel have a high strength-to-cost ratio, and thus it has a high potential to be widely applied in construction industry to reduce the construction and life-long cost. Ferritic stainless steel has been used as construction material in buildings, houses, roofing of large-span structures and bridges in Europe, Japan and South Africa [1]. Fire is a potential hazard in these applications. Further structural applications of ferritic stainless steels have been investigated in a Research Fund for Coal and Steel (RFCS) project of "Structural Applications of Ferritic Stainless Steels (SAFSS)" [2], which develops design guidelines and technical information sheet for engineers and architects to use ferritic stainless steel in structural components. Therefore, it is important to evaluate the structural performance of stainless steel structures after exposed to fire hazards, considering the high initial cost of stainless steel structures. The objectives of this research are to provide new test data and also propose design equations to predict the residual factors of mechanical properties and stress-strain relationship after exposed to fire. The investigation on their post-fire mechanical properties provides evidence in repair and reinforcement of stainless steel structures after fire hazards, and thus reduce economic losses of fire and improve sustainability of the built environment. The relevant results and analytical models can be referred to in the fire engineering design of stainless steel structure.

Residual mechanical properties of steel materials in post-fire condition have been investigated by previous researchers, including high strength structural steel of grade S460, S690 and S960 [3, 4], structural steel and reinforcing steel [5], cold-formed steel of grades G300, G500 and G550 [6], NiTi shape memory alloy [7], and austenitic stainless steel [8]. After a steel structure is exposed to fire, the steel members can be cooled down at a wide range of cooling rates. It is impossible to control or

predict these cooling rates in the real fire situations. The effect of cooling rate on carbon steel has been investigated by previous researchers [5, 9, 10]. It has shown that the stress-strain curves of carbon steel specimens that are cooled in furnace, cooled in blanket and cooled in air are almost the same. The yield strength of the post-fire specimens increase significantly when they are cooled in water. Previous researches [11, 12] suggested that the soak time has negligible effect on post-fire mechanical properties for carbon steel and austenitic stainless steel. However, there is no available research on post-fire mechanical properties of ferritic stainless steel. Therefore, the effect of the exposed high temperatures, cooling rate and soak time on the mechanical properties of ferritic stainless steel materials are remain unknown to the engineers.

On the other hand, numerous stress-strain models to predict the full stress-strain behavior for stainless steel material have been proposed by previous researchers. The Ramberg-Osgood equation [13] has been widely used for a rounded stress-strain curve. In recent years, some researches [14 – 16] were conducted to improve the Ramberg-Osgood model, where 2-stage models were used for a more accurate prediction. The model proposed by Rasmussen [15] has been widely used for stainless steel. Later on, the two-stage model was further modified to a three-stage model [17, 18], in which an intermediate point at 2.0% proof stress was used. Stress-strain model for cold-formed steel with yield plateau was proposed by Mander [19], and further modified by Tao et al. [5].

Experimental investigation on post-fire mechanical properties of ferritic stainless steel has been conducted and presented in this paper. A total of 58 ferritic stainless steel specimens have been tested. The ferritic stainless steel are cooled down with four different cooling methods from the specified elevated temperature to room temperature, namely cool-in-chamber (CIC), cool-in-air (CIA), cool-in-air-with-fan (CAF) and cool-in-water (CIW). Therefore, the influence of various cooling rates is investigated. It is showed that different cooling rates have negligible effect on the post-fire mechanical properties of ferritic stainless steel. The residual factors of the Young's modulus, yield strength, ultimate strength, Ramberg-Osgood parameter, strain at the ultimate strength,

hardness, and energy absorption have been obtained and reported. The ferritic stainless steel exhibits a unique post-fire mechanical behaviour, as its ultimate strength increased significantly after exposed to an elevated temperature higher than 700°C. The microstructure of the ferritic stainless steel specimens after exposed to fire has been investigated using scanning electron microscope (SEM), in order to understand the post-fire mechanical behaviour of these two materials. The residual mechanical properties of steel materials are compared with the predicted values calculated by the existing equations. It is shown that the existing design equations are not capable of providing accurate predictions for ferritic stainless steel. Design equations are proposed to predict the post-fire mechanical properties, which was then assessed by reliability analysis.

2. EXPERIMENTAL INVESTIGATION

2.1 Test Specimen

The test coupon specimens were extracted from cold-formed ferritic stainless steel (EN 1.4003 or ASTM S40977) rectangular hollow sections (RHS). The nominal dimension (D×B×t) of the sections are 100×40×2, 120×80×3 and 100×40×3, where D, B, t are the depth, width and thickness in millimeter of the cross-sections, respectively. The coupon dimension agrees with the Australian Standard (AS 1979) [20], American Standard (ASTM 2002) [21] and European Code (BS EN ISO 6892-2: 2011) [22] for the tensile testing of metals at elevated temperatures. The specimens were labeled such that the steel type, thickness, temperature that the specimens exposed to, the soak time and the cooling methods could be identified, as shown in Table 1. The first letter and the number indicates the steel type and section, where "F1", "F2" and "F3" represents coupon specimens extracted from rectangular hollow sections with nominal dimension of 100×40×2, 120×80×3 and 100×40×3, respectively. The second letter "T" represents temperature, and thus the number after "T" is the temperature that the specimen is exposed to in degree Celsius. The third letter "s" represents soak time. The number after "s" is the time for which the specimen is exposed to a specified temperature in minutes. Then the last letter represents the cooling methods of cool-in-chamber (C),

cool-in-air (A), cool-in-air-with-fan (F) and cool-in-water (W). If a test was repeated, the symbol "#" represents a repeated test. For example, the label "F3T600s20A$^{\#}$" represents a repeated ferritic stainless steel coupon specimen extracted from section 100×40×3 being exposed to 600 °C for 20 minutes, and it was cooled down in air. Specimens F1T24, F2T24 and F3T24 do not have the heating and cooling process, but be tested in tensile loading at ambient temperature after being extracted from sections.

2.2 Test Procedure

A total of 22 ferritic stainless steel specimens (type "F1" and "F2") were heated up and cooled down in an MTS high temperature furnace, which was controlled by Flex Test SE controller, as shown in Fig. 1(a). The cooling method of cool-in-chamber (CIC) was used for these specimens. The chamber is able to generate elevated temperatures up to 1400 °C with an accuracy of 1 °C. There are three heating elements located at the upper, middle and lower parts on each of the two sides of the furnace. Three internal thermal couples were installed to measure the air temperature, while another external thermal coupon was attached at the mid-length of the coupon specimen to measure the specimen temperature. A typical temperature-time relationship for a specimen during the heating and cooling process is shown in Fig 2. The coupon specimens was gripped at the upper end during the heating and cooling stage, while leaving the lower end free to expand. Thermal expansion (longitudinal strain) of each specimen during heating and cooling was monitored and recorded by a high temperature extensometer with 25 mm gauge length. The extensometer was mounted onto the specimens during heating and cooling stage. A constant heating rate of 20 °C/min is applied, until the corresponding specimen temperature reached the target temperature. The target high temperature will be maintained for a period of time (soak time). The soak time is generally 20 mins, except that specimens F2T600s0, F2T600s60 and F2T600s180 were heated for 0 min, 60 mins and 180 mins, respectively, to investigate the influence of soak time for post-fire mechanical properties. After the soak time, the heating elements stop generating heat. The specimens were left inside the chamber for

cooling down until the specimen temperature is below 150 °C, and then the specimens were took out from the chamber for further cooling down to room temperature of around 24 °C.

A total of 30 coupon specimens of type "F3" were heated in a Catterson Smith annealing oven, and cooled down to room temperature by three different cooling methods, namely cooled-in-air (CIA), cool-in-air-with-fan (CAF) and cool-in-water (CIW), as shown in Fig 1(b). The oven is able to generate elevated temperatures up to 1200 °C. Three heating elements are located on both sides and the top of the annealing oven. Two internal thermal couples at the front door and at the back hole are used to measure the air temperature, in order to control the temperatures of the heating elements. An external type K thermocouple was attached with the specimen during the heating and cooling stage to measure the specimen temperature. Fire cement is used to attach the external thermocouple with the specimen, in order to monitor the specimen temperature during the heating and cooling process, as shown in Fig 1(c). The fire cement is able to withstand temperature up to 1500 °C. A constant soak time of 20 min was applied for all specimens heated in the annealing oven. After the soak time, the heated specimens were taken out from the heat chamber and cooled down to room temperature. Ten specimens were placed on the surface of a brick and cooled down naturally (cool-in-air). An electric fan was used to speed up the cooling process for the cool-in-air-with-fan method. The rest of the heated specimens were taken directly from the annealing oven to a metal bucket filled of water for the cool-in-water method. Fig 3 shows the specimen temperature of ferritic stainless steel specimens that cooled down from 700 °C to room temperature with four different cooling methods. The cooling time at Fig 3 starts from the end of the soak time.

After the heating and cooling procedure, tensile coupon tests were then conducted at ambient temperature (24 °C) for the specimens at post-fire conditions. The test setup is shown in Fig 4. The loading machine was driven by displacement control of stroke during the tensile coupon tests. The experimental procedure described in [23] for ferritic stainless steel flat coupons was used in this

study. Tensile loading was applied to the specimens until fracture, so that the whole stress-strain curve can be obtained.

The microstructures of types “F1” and “F2” are examined by HITACHI S-3400N scanning electron microscope (SEM), in order to understand the characteristics of the tested stainless steel specimens after exposed to high temperatures. The test samples were grounded with silicon carbide grinding papers from 240 to 1200 grit, and then polished with 1.0 μm and 0.5 μm diamond compounds. Then, the samples were electrolytically etched with solution of perchloric acid (70%) and ethanol (100%) by 1:4. The microstructure of ferritic stainless steel of the scale of 50 μm are shown in Fig 5. The chemical compositions of several specimens after exposed to different elevated temperatures are obtained from energy-dispersive X-ray (SEM EDX) spectrum, as shown in Table 2.

Vickers hardness tests for types “F1” and “F2” was conducted with an ESE WAY Hardness Tester at ambient temperature, in order to investigate the influence of the exposed high temperature on hardness of ferritic stainless steel. The test method and procedure conform to European and American standards [24, 25]. A force equal to 30 kgf (294.2 N) was applied to specimens for 10 seconds. Then the lengths of the two diagonals were measured under microscope. The arithmetical mean of the two lengths was taken to determine the Vickers hardness value for each specimen, according to BS EN ISO 6507-4 [26]. The hardness values of the test specimens were summarized in Table 1 and Fig 6.

2.3 Test Result

2.3.1 Effect of elevated temperatures

The effect of elevated temperatures on various post-fire mechanical properties is summarized in Figs 7 – 13. The specimens shown in Figs 7 – 13 are heated and cooled down in chamber (CIC) with a constant soak time of 20 mins for direct comparison. The post-fire static stress-strain curves of ferritic stainless steel specimens are shown in Fig 7. It is shown that the stress-strain curves behave

differently in three temperature ranges, i.e. 24 – 400 °C, 500 – 700 °C and 800 – 1000 °C. The specimens exposed to temperatures of 24, 200, 300 and 400 °C have a rounded stress-strain curve without a yield plateau. Strength of the material does not increase much beyond 0.2% yield strength. The ratio of ultimate strength to yield strength (0.2% proof stress) for ferritic stainless steel specimens that exposed to 24, 200, 300 and 400 °C ranges between 1.05 – 1.15. Compared with specimens exposed to temperature up to 400 °C, specimens exposed to temperature of 500 – 700 °C have a much lower elastic limit, followed by a yield plateau in stress-strain curves. The strain at ultimate strength ($\varepsilon_{u,T}$) and strain at fracture ($\varepsilon_{f,T}$) of specimens exposed to temperatures of 500 – 700 °C increased, compared the specimens exposed to temperature up to 400 °C. For specimens exposed to high temperature beyond 700 °C, their strengths increase rapidly, while the strain decrease significantly. The stress-strain curve is rounded without yield plateau. A substantial increase of material strength beyond yield strength (0.2% proof stress) is observed. The ratio of ultimate strength to yield strength (0.2% proof stress) for ferritic stainless steel specimens that exposed to 800, 850, 900 and 1000 °C ranges between 1.29 – 1.39. Such rapid change of mechanical properties in this range is due to the formation of martensite, which is very hard and brittle. The formation of martensite beyond 700 °C can be observed with scanning electron microscope, as described in Section 2.3.4 of this paper.

Post-fire mechanical properties of specimens exposed to temperature T, including Young's modulus (E_T), 0.2% proof stress (yield strength) ($f_{0.2,T}$), 0.5% proof stress ($f_{0.5,T}$), 1.5% proof stress ($f_{1.5,T}$), 2.0% proof stress ($f_{2.0,T}$), ultimate strength ($f_{u,T}$), strain at ultimate strength ($\varepsilon_{u,T}$), strain at fracture ($\varepsilon_{f,T}$) and Ramberg-Osgood parameter (n_T), are summarized in Table 1. The post-fire Ramberg-Osgood parameter is calculated using $n_T = ln\ (0.01/0.2) / ln\ (f_{0.01,T}/f_{0.2,T})$, where the 0.2% proof stress ($f_{0.2,T}$) and 0.01% proof stress ($f_{0.01,T}$) are intersect points of the stress-strain curve and the proportional lines off-set by 0.2% and 0.01% strains, respectively. The $f_{0.5,T}$, $f_{1.5,T}$ and $f_{2.0,T}$ are the stresses corresponding to the specified strain levels of 0.5%, 1.5% and 2.0%, respectively. Residual

factors of test specimens, which are ratios of post-fire mechanical properties after exposed to elevated temperature T over the mechanical properties at ambient temperature (E_T/E_o, $f_{0.2,T}/f_{0.2,o}$, $f_{u,T}/f_{u,o}$, $\varepsilon_{u,T}/\varepsilon_{u,o}$ and n_T/n_o), were plotted against specimen temperatures, as shown in Figs 8 – 12. It is shown that the Young's modulus (E_T) generally remain the same with different temperatures up to 1000 °C (Fig 8), while the other mechanical properties vary with temperatures. The 0.2% proof stress ($f_{0.2,T}$), 0.5% proof stress ($f_{0.5,T}$), 1.5% proof stress ($f_{1.5,T}$), 2.0% proof stress ($f_{2.0,T}$) generally remain the same for temperatures up to 400 °C, then decrease with temperature for 400 < T < 700 °C, and then increase significantly with temperature for 700 < T < 850°C, and finally maintained the same level for 850 < T < 1000 °C, as shown in Fig 9. The residual factors of strain at ultimate ($\varepsilon_{u,T}/\varepsilon_{u,o}$) and Ramberg-Osgood parameter (n_T/n_o) for specimens after exposed to different temperatures are shown in Figs 11 and 12, respectively.

The energy absorptions for post-fire ferritic stainless steel specimens are shown in Fig 13. The energy absorption is calculated by $U_T = \int_0^{\varepsilon} f d\varepsilon$, where U_T is the total mechanical energy per unit volume absorbed by the material during the tensile testing after exposed to high temperature T; f is stress and ε is strain. The energy absorption for each specimen is summarized in Table 1. The energy absorbed by the ferritic stainless steel generally increases for $T \leq 700$ °C. However, it drops rapidly at 800°C, and increases again for $T > 800$ °C.

2.3.2 Effect of soak time

The research project also investigated the influence of soak time (heating time) on the post-fire mechanical properties. The stress-strain curves for ferritic stainless steel specimens after exposed to 600 °C with soak time of 0, 20, 60 and 180 mins are shown in Fig 14, and the corresponding mechanical properties are summarized in Table 1. It is shown that the different soak time has minimum effect on stress-strain curves of the four specimens. The Young's modulus and material strengths do not change with soak time. The strain at ultimate strength ($\varepsilon_{u,T}$) and strain at fracture ($\varepsilon_{f,T}$)

of specimens with 180 mins soak time are 17% and 9.9% larger than those with 0 min soak time. It is noted that the stress-strain curves for specimens with soak time of 60 and 180 mins are almost coincide with each other, which suggests that a longer soak time beyond 60 mins do not change the post-fire mechanical properties of ferritic stainless steel materials. However, this conclusion is drawn from a small amount of test samples, and more test results are needed to confirm the effect of soak time on post-fire mechanical properties.

2.3.3 Effect of cooling rates

The mechanical properties of the ferritic stainless steel specimens that cooled down by four different cooling methods (i.e. cool-in-chamber, cool-in-air, cool-in-air-with-fan and cool-in-water) are summarized in Table 1. The residual factors of the Young's modulus, yield strength, ultimate strength, strain at ultimate strength and Ramberg-Osgood parameter of specimens after being exposed to elevated temperatures ranging from 600 to 1000 °C for the four different cooling methods are shown in Figs 15 – 19, respectively. Generally speaking, the different cooling methods have negligible effects for Young's modulus, yield strength and ultimate strength of ferritic stainless steel specimens after being exposed to elevated temperatures ranging from 600 to 1000 °C, thus it does not affect the repair and reinforcement scheme of stainless steel structures after fire hazards. It should be noted that such behaviour is quite different from carbon steel, which exhibits an increased strength when the specimen is cooled down rapidly (i.e. cool-in-water). However, the different cooling rates affects the strain at ultimate strength ($\varepsilon_{u,T}$) of specimens after exposed to 600 to 800 °C, and Ramberg-Osgood parameter (n_T) of specimens after exposed to 600 to 700 °C, as shown in Figs 18 and 19, respectively.

2.3.4 Microstructure and chemical composition

The microstructure and chemical composition of ferritic stainless steel specimens after exposed to high temperatures are examined using scanning electron microscopy analysis. These specimens

are cooled down in chamber (CIC). The microstructure of the specimens after exposed to temperature up to 800°C mainly consists of ferrite, and the grain size of these specimens are similar. The ferrite transforms to martensite when the specimens were exposed to high temperatures of 850 - 1000°C, as shown in Fig 5. The grain structure changes from rounded ferrite grains to plated martensite grains. The grain size of martensite increases with temperature from 850 to 1000°C, as shown in Fig 5. Martensite is formed during the cooling process, and it is a very hard constituent. Therefore, the hardness and ultimate strength of ferritic stainless steel rapidly increase after the specimen was exposed to high temperature beyond 800°C. The chemical composition of ferritic stainless steel specimens generally remain the same after exposed to elevated temperatures from 24 – 1000°C.

3. EVALUATION OF EXISTING EQUATIONS

The design values predicted by previous researches on post-fire mechanical properties are compared with the test results. The total thermal expansion during the heating process for ferritic stainless steel specimens that are cooled in chamber was summarized in Table 1. The relationship between thermal expansion and specimen temperature are plotted in Fig 20. The thermal expansion predicted by the EC3 Part 1.2 [27] for austenitic stainless steel is compared with the test results in Fig 20. It should be noted that design rule for ferritic stainless steel is not available in EC3 Part 1.2 [27]. It is shown that the equation is not suitable to be used for ferritic stainless steel.

Compare with the tensile coupon tests, hardness test is much cheaper and easier to be conducted. It is a non-destructive testing technique, thus the structure does not need to be damaged to obtain the mechanical properties. The hardness value can be obtained on-site after a structure is exposed to fire hazard. Huang and Young [28] has proposed an equation to predict ultimate strength ($f_{u,T}$) at post-fire condition with the hardness value (HV) for lean duplex stainless steel, where $f_{u,T}$ = 3.4×HV - 91.9. The suitability to use this equation for ferritic stainless steel is assessed in this study. The test results and predicted values of ultimate strengths of ferritic stainless steel is plotted in Fig 21. It is shown

that the predicted values agree well with the test results. The mean value of the test-to-design ratio equal to 1.01 with coefficient of variation (COV) of 0.058. Therefore, the equation provides accurate prediction for post-fire ultimate strength of ferritic stainless steel after exposed to high temperature up to 1000 °C.

The test results of residual factors (E_T/E_o, $f_{0.2,T}/f_{0.2,o}$, $f_{u,T}/f_{u,o}$, $\varepsilon_{u,T}/\varepsilon_{u,o}$ and n_T/n_o) for the ferritic stainless steel specimens were compared with the design values calculated by the existing equations [3-6, 8], as shown in Figs 8 – 12. It is shown that the equation proposed by Wang et al. [8] is generally capable of predicting residual factors of Young's modulus (E_T/E_o) for ferritic stainless steel by taking residual factor equals to 1. However, the other existing equations are not applicable for ferritic stainless steel post-fire mechanical properties, especially for $T \geq 800$°C. Therefore, new design equations for ferritic stainless steel residual factors of $f_{0.2,T}/f_{0.2,o}$, $f_{u,T}/f_{u,o}$, $\varepsilon_{u,T}/\varepsilon_{u,o}$ are required.

4. PROPOSED DESIGN RULES

4.1 Residual Factors

The design proposal consists of two parts, residual factor (χ) and stress-strain model. An unified equation of Eq. (1),

$$\chi = a + \frac{c}{T}(T - d)^b \tag{1}$$

is adopted to predict residual factors of different post-fire mechanical properties for ferritic stainless steel materials, where a, b, c and d are parameters as summarized in Table 3, and T is the specimen temperature (°C) at soak time during heating stage. The parameters varies for different residual factors at different temperature ranges. Therefore, the unified equation can be used to predict different residual factors (E_T/E_o, $f_{0.2,T}/f_{0.2,o}$, $f_{u,T}/f_{u,o}$, $\varepsilon_{u,T}/\varepsilon_{u,o}$ and n_T/n_o) for ferritic stainless steel after exposed to temperatures up to 1000 °C. The comparison of residual factors obtained from tests and those calculated from the proposed design rule are shown in Figs 8 – 12. It is shown that the

proposed design rules are generally capable of providing accurate predictions for residual factors of ferritic stainless steel mechanical properties after exposed to fire. Therefore, the design post fire mechanical properties can be obtained by multiplying the design residual factor (χ) with the mechanical properties obtained at room temperature.

4.2 Reliability Analysis

The reliability of the proposed design rules to predict the residual mechanical properties was evaluated using reliability analysis, which is detailed in the Commentary of the ASCE [29]. A target reliability index of 2.50 for stainless steel members is adopted in this study. The resistance factors of the design rules were determined using Eq. 6.2-2 of the ASCE Specification [29]. The load combination of 1.2DL+1.6LL was used in calculating the resistance factors (ϕ) for the proposed equation for residual factor (χ), where DL is the dead load and LL is the live load. The statistical parameters M_m = 1.10, F_{ym} = 1.00, V_{ym} = 0.10 and V_F = 0.05, which are the mean values and coefficients of variation for material properties and fabrication factors for yield strength and Young's modulus in the Commentary of the ASCE Specification [29] were adopted for post-fire Young's modulus (E_T) and 0.2% proof stress ($f_{0.2,T}$). The statistical parameters M_m = 1.10, F_{um} = 1.00, V_{um} = 0.05 and V_F = 0.05 for ultimate strength in the commentary were adopted for post-fire ultimate strength, strain at ultimate strength ($\varepsilon_{u,T}$) and Ramberg-Osgood parameter (n_T). The mean value (P_m) and coefficient of variation of tested-to-predicted load ratio (V_p) are shown in Table 4. The correction factor Eq. F1.1-3 in the North American Cold-formed Steel Specification AISI S100 [30] was used to account for the influence by the number of data.

In this study, two sets of resistance factor (ϕ_0 and ϕ_1) and reliability index (β_0 and β_1) are determined, as shown in Table 4. The resistance factor (ϕ_0) is calculated based on the reliability index (β_0) of 2.50. In other words, the value of ϕ_0 is the maximum resistance factor required to achieve the target reliability index (β_0). However, a slightly smaller resistance factor (ϕ_1) that

rounded to integer or a decimal of 0.5 is recommended for practical use by engineers, as reported in Table 4. It is shown that the proposed design rules provide accurate predictions for post-fire mechanical properties of ferritic stainless steel. The mean values of χ_t/χ_d range from 1.01 to 1.03 for various post-fire mechanical properties with COV of 0.025 to 0.231 for ferritic stainless steel. The χ_t and χ_d are residual factor obtained from test results and residual factor calculated from proposed design rule, respectively. The reliability index (β_I) corresponding to the recommended resistance factors (ϕ_I) are all larger than or equal to the target reliability of 2.50. Therefore, the proposed design rules are considered to be reliable with the recommended resistance factors. It is recommended that the resistance factor of Young's modulus, yield strength, ultimate strength, strain at ultimate strength and Ramberg-Osgood parameter equal to 0.90, 0.90, 0.90, 0.85 and 0.70 for ferritic stainless steel, respectively, in order to achieve the reliability index higher than the target value of 2.5.

4.3 Stress-strain Model For Ferritic Stainless Steel

The stress-strain curves for ferritic stainless steel after exposed to high temperatures ranging from 24 ≤ T< 500 °C and 700 < T ≤ 1000 °C have a typical stainless steel round-house non-linear behaviour, while the stress-strain curves for specimens after exposed to 500 ≤ T< 700 °C exhibit yield plateau, as discussed in Section 2.3.1. Therefore, different stress-strain models for ferritic stainless steel at post-fire conditions are needed for different temperature ranges. Various existing stress-strain models for rounded stress-strain curves are reviewed. It is proposed that the two-stage model [15] for stainless steel together with the post fire mechanical properties (E_T, $f_{0.2,T}$, $f_{u,T}$, n_T, $\varepsilon_{u,T}$) calculated from the proposed design rule are used for ferritic stainless steel after exposed to 24 ≤ T< 500 or 700 < T ≤ 1000, as expressed by Eqs (1 – 3) in Table 3. For the post-fire specimens exposed to 500 ≤ T ≤ 700, it is proposed to use the basic curve developed by Tao et al. [5], as expressed by Eqs (4 – 7) in Table 3. However, the equations for $\varepsilon_{p,T}$ and $E_{p,T}$ are modified to Eq. (6) and Eq. (7) for ferritic stainless steel in Table 3, respectively, where $\varepsilon_{p,T}$ is strain at the onset of strain hardening and $E_{p,T}$ is initial modulus of elasticity at the onset of strain hardening. Therefore, the post-fire stress

strain relationship of ferritic stainless steel can be predicted by the model proposed by Tao et al. [5] together with the proposed equations for $\varepsilon_{p,T}$ and $E_{p,T}$ as well as the unified equation for post-fire residual factors proposed in this study. The proposed post-fire stress-strain model for ferritic stainless steel is summarized in Table 3. The comparison of stress-strain curves obtained from tests and calculated from design equations are shown in Fig 22. It is observed that the stress-strain curves calculated using the design equations generally compare well with the full stress-strain curves obtained from tests.

5. CONCLUSIONS

An experimental investigation of post-fire mechanical properties of ferritic stainless steel has been presented. The coupon specimens were heated and maintained at specified high temperatures up to 1000 °C for a certain soak time, and then cooled down to room temperature with different cooling methods. Tensile coupon tests were conducted on the post-fire specimens until fracture. The Young's modulus of ferritic stainless steel specimens generally remain the same after exposed to high temperatures, while the strength and hardness increase significantly after being exposed to temperatures beyond 800 °C. Formation of martensite in microstructure of specimens after exposed to temperature beyond 800 °C is observed with scanning electronic microscope. It is shown that the soak time and cooling rates have negligible effect on the strength of material, but the cooling rates affect the strain and Ramberg-Osgood parameters at a certain temperature range. Linear relationship between Vickers hardness value and ultimate strength at post-fire condition was obtained and reported. It is shown that the existing design equations are generally not applicable for ferritic stainless steel at post-fire conditions, as the existing design rules are developed mainly base on carbon steel. Design equations for residual factors of mechanical properties after fire exposure and stress-strain relationships are proposed. The design values are compared with the test results, and it is shown that the proposed design rules are capable of providing accurate predictions for the test specimens. Therefore, it is recommended that the design proposal of residual factors and post-fire

stress-strain relationship can be used for cold-formed ferritic stainless steel after exposed to high temperatures up to 1000 °C.

ACKNOWLEGEMENTS

The authors are grateful to STALA Tube Finland for supplying the test specimens. The authors are also thankful to Miss Linjie Dai, Mr. Zheyi Li, Mr. Wing Kei Ho and Mr. Hungkai Wang for their contribution in this research work as part of their undergraduate final year thesis project at the University of Edinburgh. The research work described in this paper was supported by the start-up fund for Dr Yuner Huang from the School of Engineering at University of Edinburgh, and a grant from the Research Grants Council of the Hong Kong Special Administrative Region, China (Project No. HKU718612E).

NOTATION

a = coefficient used in proposed unified equation;

B = width of cross-section;

b = coefficient used in proposed unified equation;

COV = coefficient of variation;

c = coefficient used in proposed unified equation;

D = depth of cross-section;

d = coefficient used in proposed unified equation;

E_o = initial Young's modulus at room temperature;

$E_{p,T}$ = initial modulus of elasticity at the onset of strain hardening

E_T = initial Young's modulus at temperature T ºC;

F_{um} = mean value of fabrication factor for ultimate strength;

F_{ym} = mean value of fabrication factor for yield strength and Young's modulus;

f = stress

$f_{u,o}$ = ultimate strength at room temperature;

$f_{u,T}$ = ultimate strength at temperature T ºC;

$f_{0.01,T}$ = strength at 0.01% strain at temperature T ºC;

$f_{0.2,o}$ = yield strength at room temperature;

$f_{0.2,T}$ = yield strength at temperature T ºC;

$f_{0.5,T}$ = strength at 0.5% strain at temperature T ºC;

$f_{1.5,T}$ = strength at 1.5% strain at temperature T ºC;

$f_{2.0,T}$ = strength at 2.0% strain at temperature T ºC;

HV = Vickers hardness value;

M_m = mean value of material factor;

m_T = parameter in stress-strain model;

n_o = Ramberg-Osgood parameter at room temperature;

n_T = Ramberg-Osgood parameter at elevated temperature T ºC;

P_m = mean value of tested-to-predicted load ratio;

p = parameter in the proposed stress-strain model;

T = temperature in ºC;

t = thickness of cross-section;

U_T = total mechanical energy per unit volume;

V_F = coefficient of variation of fabrication factor;

V_p = coefficient of variation of tested-to-predicted load ratio;

V_{um} = coefficient of variation of material factor for ultimate strength;

V_{ym} = coefficient of variation of material factor for yield strength and Young's modulus;

β_0 = reliability index;

β_1 = reliability index;

χ = residual factor;

χ_d = residual factor calculated from proposed design rule;

χ_t = residual factor obtained from test results;

ε = strain;

$\varepsilon_{f,T}$ = tensile strain at fracture at temperature T ºC;

$\varepsilon_{p,T}$ = strain at the onset of strain hardening;

$\varepsilon_{u,o}$ = tensile strain at ultimate strength at room temperature; and

$\varepsilon_{u,T}$ = tensile strain at ultimate strength at temperature T ºC.

ϕ = resistance factor;

ϕ_0 = resistance factor; and

ϕ_1 = resistance factor.

REFERENCE

[1] "The Ferritic Solution – Properties, Advantages, Applications" (2007). International Stainless Steel Forum (ISSF).

[2] "Structural Applications of Ferritic Stainless Steel (SAFSS)" (2010). Research Fund for Coal and Steel (RFSR-CT-2010-00026), European Commission.

[3] Qiang, X., Bijlaard, F. and Kolstein, H. (2012). "Post-fire mechanical properties of high strength structural steels S460 and S690", *Engineering Structures*, 35, pp.1-10.

[4] Qiang, X., Bijlaard, F. and Kolstein, H. (2013). "Post-fire performance of very high strength steel S960", *Journal of Constructional Steel Research*, 80, pp.235-242.

[5] Tao, Z., Wang, X-Q., and Uy, B. (2013). "Stress-strain curves of structural and reinforcing steels after exposure to elevated temperatures." *Journal of Materials in Civil Engineering*, ASCE, 25(9), 1306-1316.

[6] Gunalan, S. and Mahendran, M. (2014). "Experimental investigation of post-fire mechanical properties of cold-formed steels." *Thin-Walled Structures*, 84, 241-254.

[7] Fang H., Wong M.B., Bai Y., Luo R. "Effect of heating/cooling rates on the material properties of NiTi wires for civil structural applications" *Journal of Construction and Building Materials*, 101(1): 447-455.

[8] Wang, X. -Q., Tao, Z., Song, T. –Y., Han, L. –H. (2014) "Stress-strain model of austenitic stainless steel after exposure to elevated temperatures", *Journal of Constructional Steel Research*, 99, pp. 1483 – 1488.

[9] Neves, I., Rodrigues, J., and Loureiro, A. (1996). "Mechanical Properties of Reinforcing and Prestressing Steels after Heating." *Journal of Materials in Civil Engineering*, ASCE, 8(4), 189-194.

[10] Outinen, J. and Mäkeläinen, P. (2004). "Mechanical properties of structural steel at elevated temperatures and after cooling down." *Fire and Materials*, 28(2-4), 237–251.

[11] Smith, C., Kirby, B., Lapwood, D., Cole, K., Cunningham, A., and Preston, R. (1981). "The reinstatement of fire damaged steel framed structures. *Fire Safety Journal*, 4(1), 21-62.

[12] Tokunaga, Y., Furukawa, N., Sakai, H., Taguchi, Y., Arima, T., and Tokura, Y. (2009). "Composite domain walls in a multiferroic perovskite ferrite." *Nature Materials*, 8(7), 558-562.

[13] Ramberg, W. and Osgood, W. R. (1943), "Description of Stress-Strain-Curves by Three Parameters" Technical Report, *Technical Note No. 902*, NACA.

[14] Mirambell, E. and Real, E., (2000) "On the calculation of deflections on structural stainless steel beams: An experimental and numerical investigation" *Journal of Constructional Steel Research*, 54 (1), pp. 109 – 133.

[15] Rasmussen, K.J.R. (2003) "Full-range stress-strain curves for stainless steel alloys" *Journal of Constructional Steel Research*, 59, pp. 47 – 61.

[16] Gardner, L. and Nethercot, D.A. (2004). "Experiments on stainless steel hollow sections - Part 1: Material and cross-sectional behaviour", *Journal of Constructional Steel Research*, 60(9), pp. 1291–1318.

[17] Quach, W.M., Teng, J.G. and Chung, K.F. (2008). "Three-stage full range stress-strain model for stainless steels", *Journal of Structural Engineering, ASCE*, 134(9), pp. 1518–1527.

[18] Hradil, P., Talja, A., Real, E., Mirambell, E., Rossi, B. (2013). "Generalized multistage mechanical model for nonlinear metallic materials", *Thin-Walled Structures*, 63, pp. 63 – 69.

[19] Mander, J. B. (1983). "Seismic design of bridge piers." *Ph.D. thesis*, Department of Civil Engineering, University of Canterbury, Christchurch, New Zealand.

[20] AS (1979). "Methods for the tensile testing of metals at elevated temperatures." *Australian Standard AS 2291*, Standard Association of Australia, Australia.

[21] ASTM (2002). "Standard test methods for elevated temperature tension tests of metallic materials." *E21*, ASTM, West Conshohocken, PA, USA.

[22] BS (2011). "Metallic materials – Tensile testing, Part 2: Method of test at elevated temperature." *BS EN ISO 6892-2: 2011*, British Standard Institution (BSI), London, UK.

[23] Huang, Y. and Young, B. (2014). "The art of coupon tests." *Journal of Constructional Steel Research*, 96, 159-175.

[24] BS (2005). "Metallic materials – Vickers hardness test – Part 1: Test method." *BS EN ISO 6507-1*, British Standard Institution (BSI), London, UK.

[25] ASTM (2011). "Standard test method for Knoop and Vickers hardness of materials." *E 384-11*, ASTM, West Conshohocken, PA, USA.

[26] BS (2005). "Metallic materials – Vickers hardness test – Part 4: Tables of hardness values." *BS EN ISO 6507-4*, British Standard Institution (BSI), London, UK.

[27] EC3. (2005). "Design of steel structures – part 1–2: general rules – structural fire design", *European committee for standardization*, EN 1993-1-2. Brussels: CEN.

[28] Huang Y., Young B. "Mechanical properties of lean duplex stainless steel at post-fire condition" *Thin-Walled Structures* (Under review).

[29] ASCE. (2002) "Specification for the design of cold-formed stainless steel structural members", *SEI/ASCE 8-02*. Reston, VA: American Society of Civil Engineers.

[30] AISI S100. (2016) "North American specification for the design of cold-formed steel structural members", *North American cold-formed steel specification*. Washington DC: American Iron and Steel Institute.

TABLE 1. Post-fire mechanical properties of ferritic stainless steel

Specimen	T (°C)	Thermal expansion (%)	E_T (GPa)	$f_{0.2,T}$ (MPa)	$f_{0.5,T}$ (MPa)	$f_{1.5,T}$ (MPa)	$f_{2.0,T}$ (MPa)	$f_{u,T}$ (MPa)	$\varepsilon_{u,T}$ (%)	$\varepsilon_{f,T}$ (%)	n_T	U_T (MPa)	HV30 (kgf/mm^2)
F1T24	24.0	0.0	214.3	460.8	464.4	469.1	470.0	483.9	12.7	26.3	7.7	122.1	168.8
F1T200s20-C	196.3	0.3	221.7	452.9	459.9	470.5	474.2	506.3	12.0	28.7	10.4	137.3	176.8
F1T300s20-C	304.5	0.3	225.6	486.8	491.8	512.2	519.1	533.5	11.6	27.3	12.5	136.8	183.2
F1T400s20-C	414.2	0.5	222.4	470.9	474.2	493.4	500.9	525.4	9.8	22.7	14.5	110.0	183.2
F1T500s20-C	498.1	0.6	221.6	402.1	406.0	428.8	442.4	507.4	11.1	26.3	28.2	123.1	187.3
F1T600s20-C	597.3	0.7	215.8	322.1	324.1	355.4	369.8	488.3	16.7	34.3	52.3	153.7	169.4
F1T700s20-C	691.9	2.6	223.3	302.8	306.6	340.9	358.7	486.5	17.5	34.6	29.3	153.5	149.5
F1T800s20-C	796.0	1.1	213.2	423.0	444.9	545.9	568.0	586.9	3.4	10.1	5.6	50.3	276.0
F1T850s20-C	864.4	0.9	214.8	767.7	717.0	965.0	980.0	1003.3	3.8	10.6	3.7	116.1	318.0
F1T900s20-C	898.2	3.3	219.6	773.8	741.6	995.9	1018.5	1038.4	4.1	12.1	3.8	108.3	305.0
F1T1000s20-C	997.7	1.1	217.6	726.8	705.0	940.2	959.7	970.4	3.2	8.5	3.0	74.4	297.0
F2T24	24.0	0.0	210.0	410.2	418.2	426.9	431.0	465.5	13.4	25.9	6.7	114.5	167.1
F2T200s20-C	203.1	0.2	216.5	424.8	433.1	446.8	450.3	483.1	13.0	28.0	7.4	124.7	175.5
F2T300s20-C	296.0	0.3	223.1	445.0	448.2	456.9	463.1	499.6	13.3	27.0	12.4	123.4	193.6
F2T400s20-C	395.3	1.2	220.3	432.4	437.5	458.9	467.6	498.8	11.6	25.9	14.2	118.4	165.9
F2T500s20-C	503.8	0.6	219.3	370.2	370.6	394.2	406.5	484.3	12.8	26.4	18.1	115.3	169.4
F2T600s0-C	620.8	0.7	215.0	324.3	325.7	352.3	368.0	473.1	14.8	26.9	42.8	113.2	155.6
F2T600s20-C	602.3	0.7	217.3	315.3	305.1	337.9	354.7	475.8	15.6	27.5	51.0	115.9	171.2
F2T600s60-C	596.6	0.7	216.7	310.6	310.2	344.9	360.7	474.7	16.4	30.1	26.9	127.9	159.3
F2T600s180-C	598.6	0.7	217.8	299.8	298.5	331.8	348.9	467.6	17.7	30.1	63.6	126.3	167.7
F2T700s20-C	703.5	0.7	220.4	291.5	292.4	324.7	341.5	464.7	17.1	30.6	27.1	126.8	159.8
F2T850s20-C	851.7	0.8	211.7	738.8	709.9	945.3	963.6	976.1	2.9	11.0	3.7	88.0	309.0
F2T900s20-C	898.3	0.7	212.5	744.3	712.6	931.3	951.6	969.8	3.5	11.5	3.7	92.1	321.0
F2T1000s20-C	989.4	0.9	205.4	762.3	720.4	949.1	967.6	975.5	2.8	10.9	4.5	86.4	308.0
F3T24	23.4	---	202.5	447.8	454.0	457.5	454.6	450.0	7.6	---	13.2	---	---
F3T24$^{\#}$	23.4	---	195.4	446.6	452.7	457.9	456.0	450.0	7.9	---	8.3	---	---
F3T24$^{\#}$	23.6	---	212.4	466.5	472.4	475.8	470.6	476.4	12.4	---	13.9	---	---
F3T24$^{\#}$	23.2	---	203.6	466.3	473.2	469.2	474.0	480.7	10.5	---	11.0	---	---

F3T600s20-A	596.6	---	200.5	330.4	333.0	355.7	368.5	441.9	7.5	---	27.5	---	---
F3T600s20-A#	585.7	---	199.2	342.2	347.4	370.1	382.9	462.3	7.7	---	25.3	---	---
F3T600s20-F	595.3	---	203.1	354.4	357.0	377.9	390.1	456.6	10.4	---	29.6	---	---
F3T600s20-F#	589.6	---	200.3	342.9	345.9	365.2	378.0	460.3	8.9	---	27.9	---	---
F3T600s20-W	593.7	---	204.2	336.5	341.4	368.4	381.8	447.7	15.6	---	13.2	---	---
F3T600s20-W#	597.1	---	201.8	352.9	363.2	394.0	406.1	469.7	14.7	---	9.4	---	---
F3T700s20-A	695.4	---	197.4	300.0	301.1	323.0	336.8	439.0	17.4	---	73.3	---	---
F3T700s20-A#	698.2	---	200.9	327.8	339.7	403.1	421.0	456.0	15.7	---	75.4	---	---
F3T700s20-F	687.7	---	199.5	333.7	335.2	358.8	372.4	468.9	20.1	---	66.3	---	---
F3T700s20-F#	689.5	---	201.1	313.2	314.2	336.6	350.6	448.5	18.9	---	60.1	---	---
F3T700s20-W	699.3	---	206.2	335.0	340.5	367.3	379.8	470.8	22.1	---	25.6	---	---
F3T700s20-W#	687.4	---	203.4	341.8	350.5	385.0	400.3	493.9	22.1	---	22.8	---	---
F3T800s20-A	798.6	---	196.7	503.3	524.5	655.5	677.1	715.4	5.9	---	4.5	---	---
F3T800s20-A#	784.6	---	200.6	503.7	517.0	622.9	642.7	688.9	5.4	---	6.1	---	---
F3T800s20-F	805.6	---	200.9	509.6	528.9	666.5	685.3	725.6	8.0	---	3.9	---	---
F3T800s20-F#	800.3	---	201.6	509.9	526.7	644.1	660.8	694.9	7.6	---	5.2	---	---
F3T800s20-W	809.6	---	202.6	533.0	557.5	687.3	703.6	723.9	7.1	---	3.6	---	---
F3T800s20-W#	796.8	---	206.4	526.4	549.7	703.0	717.6	746.7	6.2	---	2.7	---	---
F3T900s20-A	900.5	---	198.5	733.3	690.7	866.8	878.5	886.2	3.8	---	5.4	---	---
F3T900s20-A#	907.3	---	202.7	724.6	693.1	868.1	882.2	888.1	2.6	---	5.3	---	---
F3T900s20-F	896.4	---	200.8	760.9	714.3	896.5	907.8	917.6	3.8	---	4.1	---	---
F3T900s20-F#	913.3	---	204.7	759.8	722.8	880.8	890.4	893.3	2.5	---	4.0	---	---
F3T900s20-W	890	---	205.6	766.7	720.7	898.7	908.0	918.3	4.1	---	4.1	---	---
F3T900s20-W#	899.5	---	206.7	783.0	742.8	887.0	895.6	897.8	3.3	---	5.8	---	---
F3T1000s20-A	1002.8	---	198.5	722.3	685.5	879.5	892.9	898.5	2.9	---	3.4	---	---
F3T1000s20-A#	998.6	---	200.0	756.3	725.7	872.4	872.4	887.7	2.0	---	4.0	---	---
F3T1000s20-F	994.6	---	200.8	723.0	688.0	872.0	883.0	885.7	2.5	---	4.5	---	---
F3T1000s20-F#	1007.5	---	204.7	758.2	723.7	874.4	882.3	888.4	2.5	---	4.5	---	---
F3T1000s20-W	1001.7	---	205.6	750.5	713.9	885.2	894.5	897.7	2.5	---	3.8	---	---
F3T1000s20-W#	987.3	---	206.7	779.3	741.2	881.9	888.3	886.9	2.7	---	5.5	---	---

Note: F1, F2 and F3 are extracted from sections 100×40×2, 120×80×3 and 100×40×3, respectively;

The last letters “C”, “A”, “F” and “W” indicate that the cooling methods are cool-in-chamber, cool-in-air, cool-in-air-with-fan and cool-in-water, respectively.

TABLE 2. Chemical composition of ferritic stainless steel specimens

Specimen	C	Si	Cr	Mn	Fe
F2T24	1.47	0.40	11.78	1.56	84.79
F2T200t20-C	1.88	0.30	11.53	1.59	84.70
F2T300t20-C	2.24	0.41	11.21	1.62	84.52
F2T600t20-C	2.29	0.32	11.31	1.45	84.63
F2T700t20-C	1.76	0.29	11.44	1.59	84.93

TABLE 3. Proposed post-fire mechanical properties for ferritic stainless steel

Residual factor $\chi = a + \frac{c}{T}(T-d)^b$	a	b	c	d	Temperature, T (°C)
$\frac{E_T}{E_o}$	1	0	0	0	$24 \le T \le 1000$
$\frac{f_{0.2,T}}{f_{0.2,o}}$	1	0	0	0	$24 \le T \le 400$
	1	1.45	-7.14E-02	400	$400 < T \le 650$
	0.67	3	1.09E-04	650	$650 < T \le 850$
	1.7	0	0	0	$850 < T \le 1000$
$\frac{f_{u,T}}{f_{u,o}}$	1	0	0	0	$24 \le T \le 700$
	1	3.5	2.22E-05	700	$700 < T \le 850$
	2.08	0	0	0	$850 < T \le 1000$
$\frac{\varepsilon_{u,T}}{\varepsilon_{u,o}}$	1	3	-1.50E-06	24	$24 \le T \le 400$
	0.8	2	4.67E-03	400	$400 < T \le 700$
	1.35	1	-8.40	700	$700 < T \le 800$
	0.25	0	0	0	$800 < T \le 1000$
$\frac{n_T}{n_o}$	1	4.8	2.06E-10	24	$24 \le T \le 600$
	7.1	0.7	-117.96	600	$600 < T \le 850$
	0.48	0	0	0	$850 < T \le 1000$

Stress-strain model:

$$\varepsilon = \frac{f}{E_T} + 0.002\left(\frac{f}{f_{0.2,T}}\right)^{n_T} \quad \text{for } f \le f_{0.2,T}$$

$$= \frac{f - f_{0.2,T}}{E_{0.2,T}} + \varepsilon_{u,T}\left(\frac{f - f_{0.2,T}}{f_{u,T} - f_{0.2,T}}\right)^{m_T} + 0.002 + \frac{f_{0.2,T}}{E_T} \quad \text{for } f_{0.2,T} < f \le f_{u,T} \qquad (1)$$

$$E_{0.2,T} = \frac{E_T}{1 + 0.002 n_T E_T / f_{0.2,T}} \qquad (2); \qquad m_T = 1 + 3.5\frac{f_{0.2,T}}{f_{u,T}} \qquad (3)$$

$24 \le T < 500$ or $700 < T \le 1000$

$$\varepsilon = \frac{f}{E_T} \quad \text{for } f < f_{0.2,T}$$

$$= \varepsilon_{u,T} - \left(\varepsilon_{u,T} - \varepsilon_{p,T}\right)\left(\frac{f_{u,T} - f}{f_{u,T} - f_{y,T}}\right)^{\frac{1}{p}} \quad \text{for } f_{0.2,T} < f \le f_{u,T} \qquad (4)$$

where

$$p = \frac{E_{p,T}\left(\varepsilon_{u,T} - \varepsilon_{p,T}\right)}{f_{u,T} - f_{y,T}} \qquad (5);$$

$$\varepsilon_{p,T} = \varepsilon_{y,T}(0.0061T + 1.0535) \qquad (6); \qquad E_{p,T} = E_T(2\times10^{-5}T + 0.0028) \qquad (7)$$

$500 \le T \le 700$

TABLE 4. Comparison of residual factors obtained from test results with design values for ferritic stainless steel

Specimen	T (°C)	χ_t					χ_d					$\frac{\chi_t}{\chi_d}$				
		E_T	$f_{0.2,T}$	$f_{u,T}$	$\varepsilon_{u,T}$	n_T	E_T	$f_{0.2,T}$	$f_{u,T}$	$\varepsilon_{u,T}$	n_T	E_T	$f_{0.2,T}$	$f_{u,T}$	$\varepsilon_{u,T}$	n_T
F1T24	24.3	1.00	1.00	1.00	1.00	1.00	1.00	1.00	1.00	1.00	1.00	1.00	1.00	1.00	1.00	1.00
F1T200t20-C	196.3	1.03	0.98	1.05	0.94	1.36	1.00	1.00	1.00	0.96	1.06	1.03	0.98	1.05	0.98	1.28
F1T300t20-C	304.5	1.05	1.06	1.10	0.91	1.63	1.00	1.00	1.00	0.89	1.38	1.05	1.06	1.10	1.02	1.18
F1T400t20-C	414.2	1.04	1.02	1.09	0.77	1.89	1.00	0.99	1.00	0.80	2.36	1.04	1.03	1.09	0.96	0.80
F1T500t20-C	498.1	1.03	0.87	1.05	0.87	3.67	1.00	0.89	1.00	0.89	3.89	1.03	0.98	1.05	0.98	0.95
F1T600t20-C	597.3	1.01	0.70	1.01	1.31	6.80	1.00	0.75	1.00	1.10	6.99	1.01	0.94	1.01	1.19	0.97
F1T700t20-C	691.9	1.04	0.66	1.01	1.37	3.82	1.00	0.68	1.00	1.37	3.06	1.04	0.96	1.01	1.00	1.25
F1T800t20-C	796.0	1.00	0.92	1.21	0.27	0.73	1.00	1.10	1.24	0.34	1.14	1.00	0.84	0.98	0.80	0.64
F1T850t20-C	864.4	1.00	1.67	2.07	0.30	0.48	1.00	1.70	2.08	0.25	0.48	1.00	0.98	1.00	1.20	0.99
F1T900t20-C	898.2	1.02	1.68	2.15	0.32	0.49	1.00	1.70	2.08	0.25	0.48	1.02	0.99	1.03	1.27	1.03
F1T1000t20-C	997.7	1.02	1.58	2.01	0.25	0.39	1.00	1.70	2.08	0.25	0.48	1.02	0.93	0.96	1.00	0.82
F2T24	22.9	1.00	1.00	1.00	1.00	1.00	1.00	1.00	1.00	1.00	1.00	1.00	1.00	1.00	1.00	1.00
F2T200t20-C	203.1	1.03	1.04	1.04	0.97	1.10	1.00	1.00	1.00	0.96	1.07	1.03	1.04	1.04	1.01	1.04
F2T300t20-C	296.0	1.06	1.08	1.07	0.99	1.84	1.00	1.00	1.00	0.90	1.34	1.06	1.08	1.07	1.11	1.38
F2T400t20-C	395.3	1.05	1.05	1.07	0.87	2.11	1.00	1.00	1.00	0.81	2.13	1.05	1.05	1.07	1.08	0.99
F2T500t20-C	503.8	1.04	0.90	1.04	0.95	2.68	1.00	0.88	1.00	0.90	4.02	1.04	1.02	1.04	1.06	0.67
F2T600s0-C	620.8	1.02	0.79	1.02	---	---	1.00	0.71	1.00	---	---	1.02	1.11	1.02	---	---
F2T600t20-C	602.3	1.03	0.77	1.02	1.16	7.57	1.00	0.74	1.00	1.12	6.75	1.03	1.04	1.02	1.04	1.12
F2T600s60-C	596.6	1.03	0.76	1.02	---	---	1.00	0.75	1.00	---	---	1.03	1.01	1.02	---	---
F2T600s180-C	598.6	1.04	0.73	1.00	---	---	1.00	0.74	1.00	---	---	1.04	0.98	1.00	---	---
F2T700t20-C	703.5	1.05	0.71	1.00	1.28	4.03	1.05	0.71	1.00	1.28	4.03	1.05	1.02	1.00	0.98	1.45
F2T850t20-C	851.7	1.01	1.80	2.10	0.22	0.55	1.01	1.80	2.10	0.22	0.55	1.01	1.06	1.01	0.87	1.15
F2T900t20-C	898.3	1.01	1.81	2.08	0.26	0.54	1.01	1.81	2.08	0.26	0.54	1.01	1.07	1.00	1.04	1.13
F2T1000t20-C	989.4	0.98	1.86	2.10	0.21	0.67	0.98	1.86	2.10	0.21	0.67	0.98	1.09	1.01	0.84	1.39
F3T24	23.4	1.00	1.00	1.00	1.00	1.00	1.00	1.00	1.00	1.00	1.00	1.00	1.00	1.00	---	---
F3T600s20-A	596.6	0.99	0.72	0.98	0.78	2.37	1.00	0.75	1.00	1.10	6.96	0.99	0.97	0.98	---	---
F3T600s20-A#	585.7	0.98	0.75	1.03	0.80	2.18	1.00	0.76	1.00	1.07	6.54	0.98	0.98	1.03	---	---
F3T600s20-F	595.3	1.00	0.78	1.01	1.09	2.55	1.00	0.75	1.00	1.10	6.91	1.00	1.04	1.01	---	---
F3T600s20-F#	589.6	0.98	0.75	1.02	0.92	2.41	1.00	0.76	1.00	1.08	6.69	0.98	0.99	1.02	---	---
F3T600s20-W	593.7	1.00	0.74	0.99	1.63	1.14	1.00	0.75	1.00	1.09	6.85	1.00	0.98	0.99	---	---

F3T600s20-W[#]	597.1	0.99	0.77	1.04	1.53	0.81	1.00	0.75	1.00	1.10	6.98	0.99	1.04	1.04	---	---
F3T700s20-A	695.4	0.97	0.66	0.98	1.81	6.32	1.00	0.68	1.00	1.39	2.98	0.97	0.96	0.98	---	---
F3T700s20-A[#]	698.2	0.99	0.72	1.01	1.64	6.51	1.00	0.69	1.00	1.39	2.91	0.99	1.04	1.01	---	---
F3T700s20-F	687.7	0.98	0.73	1.04	2.10	5.72	1.00	0.68	1.00	1.36	3.17	0.98	1.08	1.04	---	---
F3T700s20-F[#]	689.5	0.99	0.69	1.00	1.97	5.19	1.00	0.68	1.00	1.37	3.12	0.99	1.01	1.00	---	---
F3T700s20-W	699.3	1.01	0.73	1.05	2.31	2.21	1.00	0.69	1.00	1.40	2.88	1.01	1.06	1.05	---	---
F3T700s20-W[#]	687.4	1.00	0.75	1.10	2.31	1.97	1.00	0.68	1.00	1.36	3.18	1.00	1.10	1.10	---	---
F3T800s20-A	798.6	0.97	1.10	1.59	0.61	0.39	1.00	1.12	1.26	0.31	1.10	0.97	0.98	1.26	---	---
F3T800s20-A[#]	784.6	0.99	1.10	1.53	0.56	0.53	1.00	1.01	1.16	0.44	1.30	0.99	1.09	1.32	---	---
F3T800s20-F	805.6	0.99	1.12	1.61	0.84	0.34	1.00	1.18	1.33	0.25	1.01	0.99	0.94	1.21	---	---
F3T800s20-F[#]	800.3	0.99	1.12	1.54	0.80	0.45	1.00	1.13	1.28	0.25	1.08	0.99	0.98	1.21	---	---
F3T800s20-W	809.6	1.00	1.17	1.61	0.74	0.31	1.00	1.22	1.38	0.25	0.96	1.00	0.96	1.17	---	---
F3T800s20-W[#]	796.8	1.01	1.15	1.66	0.65	0.24	1.00	1.10	1.25	0.33	1.13	1.01	1.04	1.33	---	---
F3T900s20-A	900.5	0.98	1.61	1.97	0.39	0.47	1.00	1.70	2.08	0.25	0.48	0.98	0.94	0.95	---	---
F3T900s20-A[#]	907.3	1.00	1.59	1.97	0.27	0.46	1.00	1.70	2.08	0.25	0.48	1.00	0.93	0.95	---	---
F3T900s20-F	896.4	0.99	1.67	2.04	0.39	0.35	1.00	1.70	2.08	0.25	0.48	0.99	0.98	0.98	---	---
F3T900s20-F[#]	913.3	1.01	1.66	1.99	0.26	0.34	1.00	1.70	2.08	0.25	0.48	1.01	0.98	0.95	---	---
F3T900s20-W	890	1.01	1.68	2.04	0.43	0.36	1.00	1.70	2.08	0.25	0.48	1.01	0.99	0.98	---	---
F3T900s20-W[#]	899.5	1.02	1.71	2.00	0.35	0.50	1.00	1.70	2.08	0.25	0.48	1.02	1.01	0.96	---	---
F3T1000s20-A	1002.8	0.98	1.58	2.00	0.30	0.30	1.00	1.70	2.08	0.25	0.48	0.98	0.93	0.96	---	---
F3T1000s20-A[#]	998.6	0.98	1.66	1.97	0.21	0.34	1.00	1.70	2.08	0.25	0.48	0.98	0.97	0.95	---	---
F3T1000s20-F	994.6	0.99	1.58	1.97	0.26	0.38	1.00	1.70	2.08	0.25	0.48	0.99	0.93	0.95	---	---
F3T1000s20-F[#]	1007.5	1.01	1.66	1.97	0.26	0.39	1.00	1.70	2.08	0.25	0.48	1.01	0.98	0.95	---	---
F3T1000s20-W	1001.7	1.01	1.64	1.99	0.26	0.33	1.00	1.70	2.08	0.25	0.48	1.01	0.97	0.96	---	---
F3T1000s20-W[#]	987.3	1.02	1.71	1.97	0.28	0.47	1.00	1.70	2.08	0.25	0.48	1.02	1.00	0.95	---	---
											# of data	55	55	55	21	21
											Mean	1.01	1.00	1.03	1.03	1.02
											COV	0.025	0.054	0.083	0.111	0.262
											Resistance factor (ϕ_0)	0.93	0.91	0.92	0.89	0.70
											Reliability index (β_0)	2.50	2.50	2.50	2.50	2.50
											Resistance factor (ϕ_1)	0.90	0.90	0.90	0.85	0.70
											Reliability index (β_1)	2.61	2.54	2.57	2.66	2.50

Note: F1, F2 and F3 are extracted from sections 100×40×2, 120×80×3 and 100×40×3, respectively;
The last letters "C", "A", "F" and "W" indicate that the cooling methods are cool-in-chamber, cool-in-air, cool-in-air-with-fan and cool-in-water, respectively.

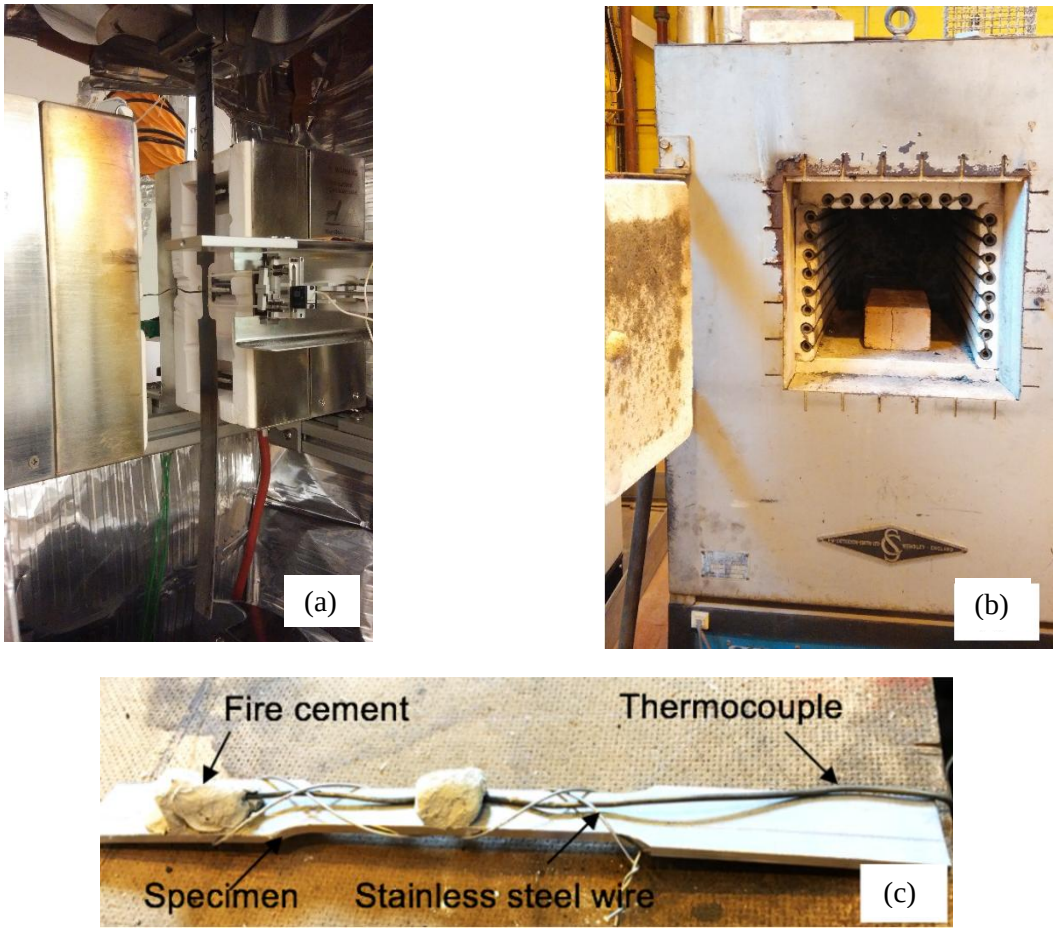

Fig. 1. (a) MTS high temperature furnace. (b) Catterson Smith annealing oven. (c) Test specimen.

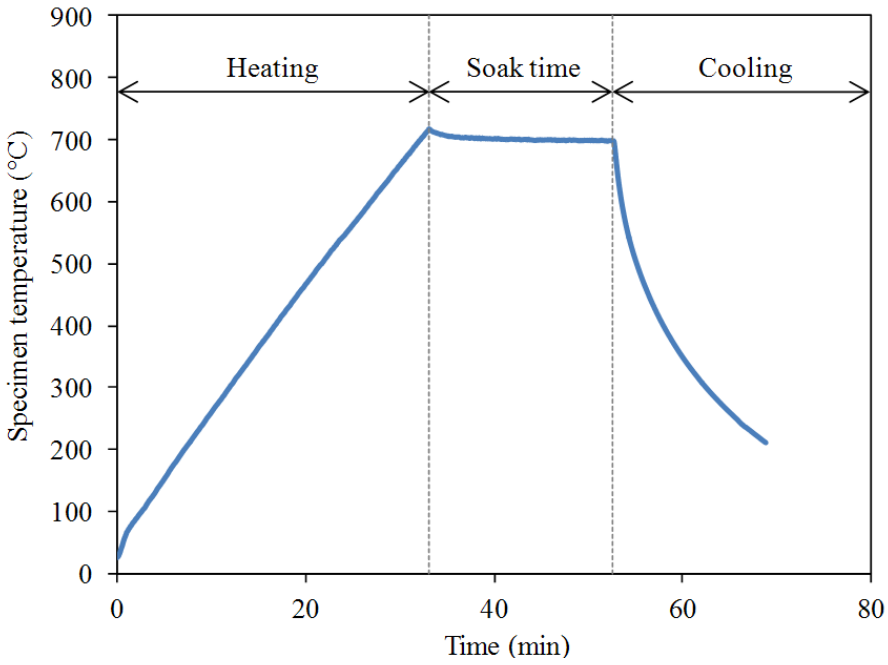

Fig. 2. Typical temperature-time relationship during heating and cooling stage.

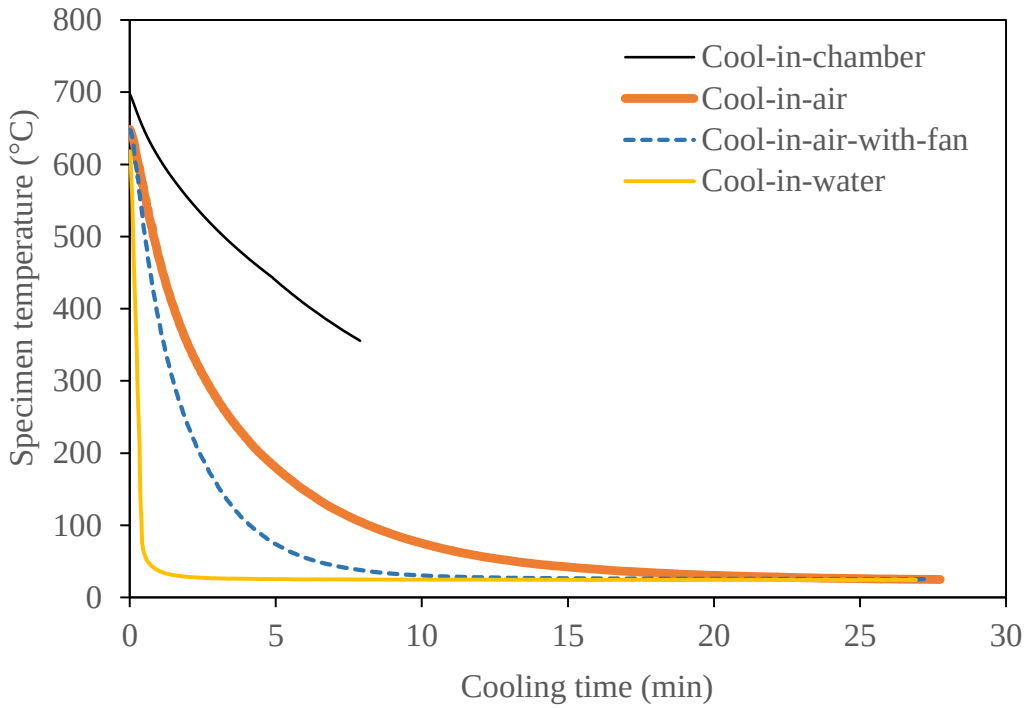

Fig. 3. Specimen temperatures in cooling stage.

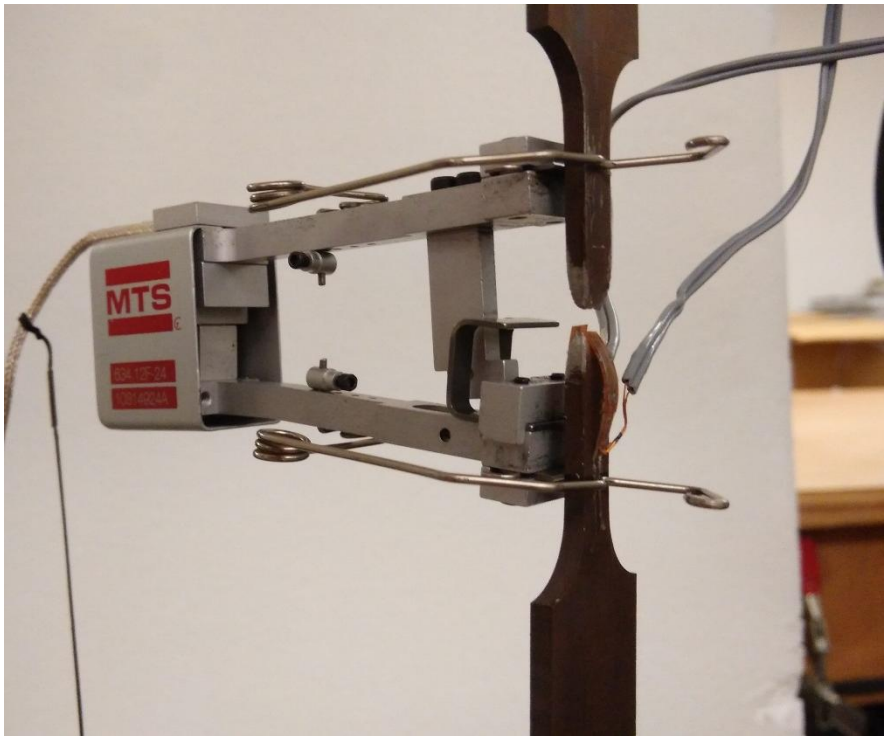

Fig. 4. Tensile coupon test for ferritic stainless steel specimen exposed to high temperature.

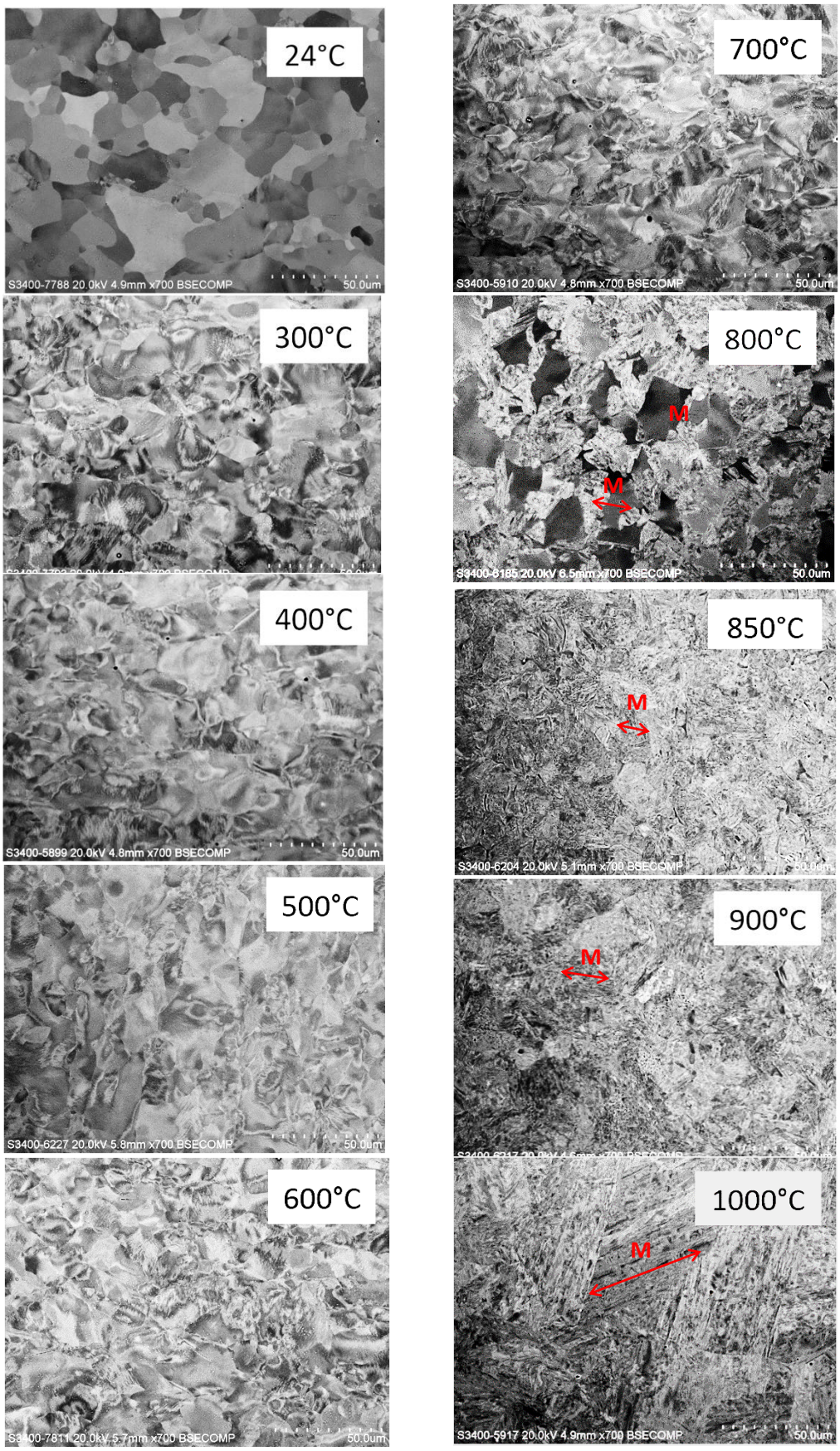

Fig. 5. Microstructure of ferritic stainless steel specimens after exposed to elevated temperatures (F = ferrite, M = martensite).

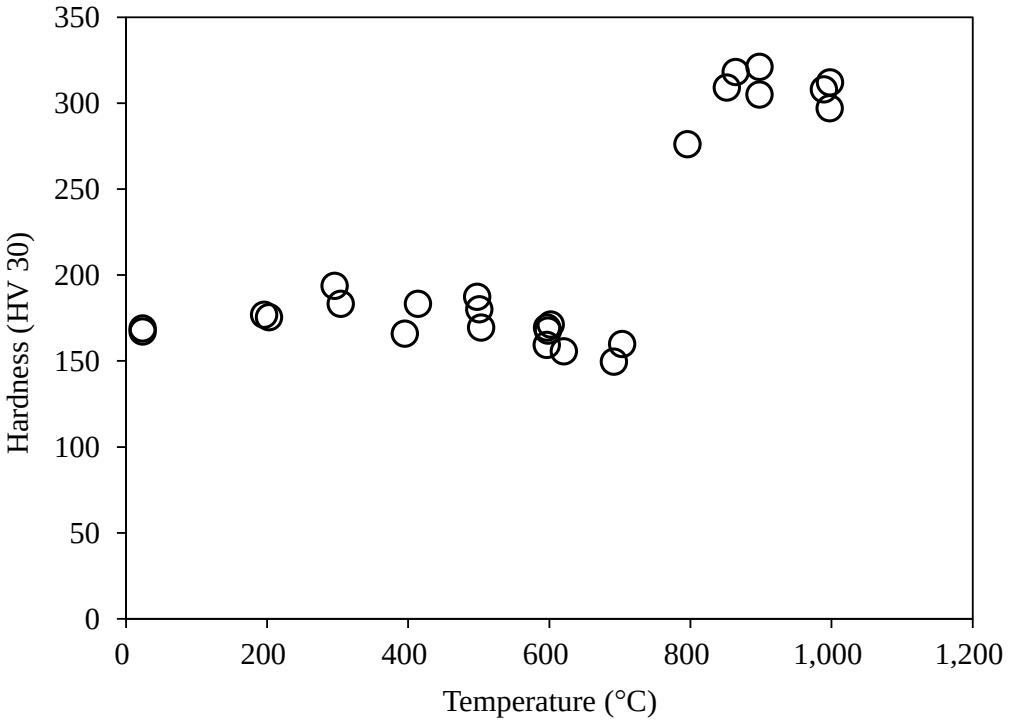

Fig. 6. Hardness of ferritic stainless steel at different temperatures.

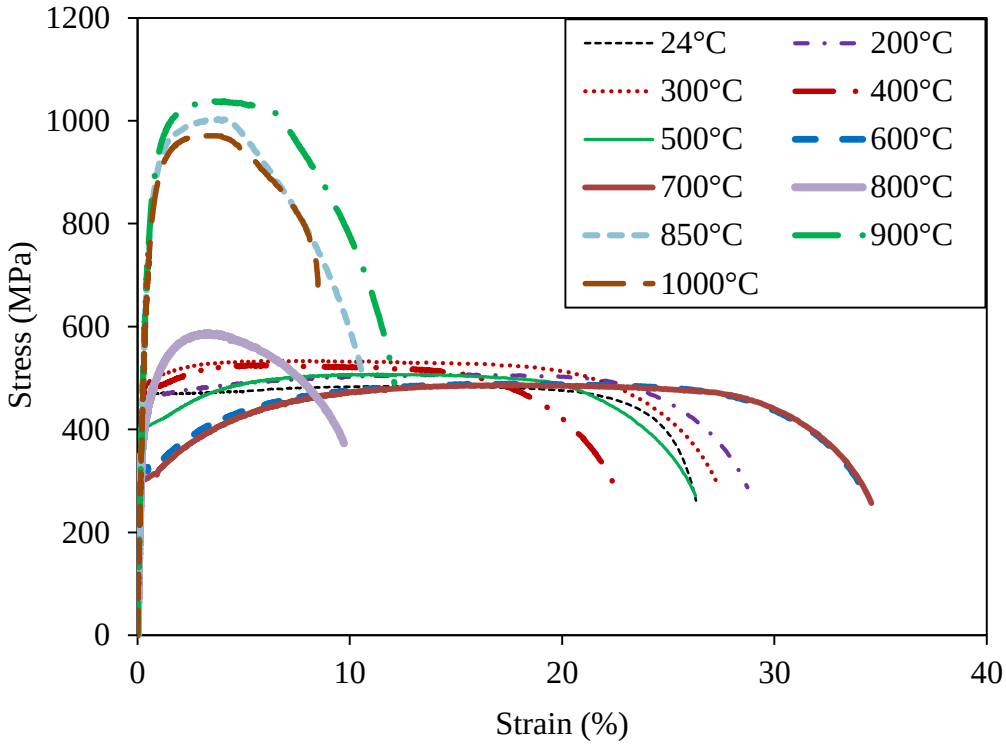

Fig. 7. Post-fire stress-strain curve of ferritic stainless steel.

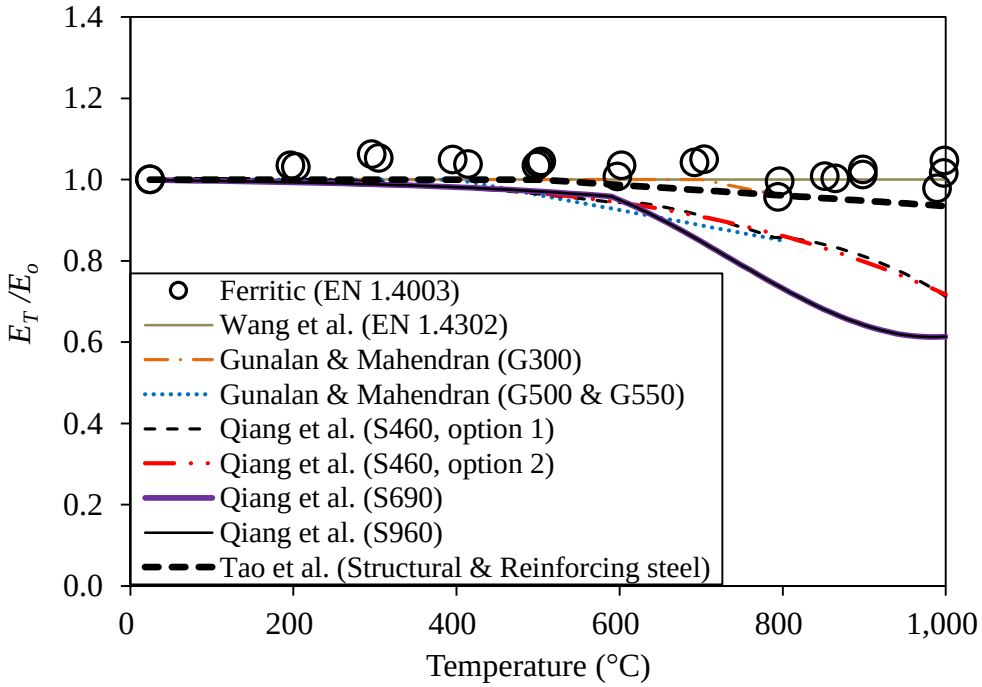

Fig. 8. Residual factor of Young's modulus.

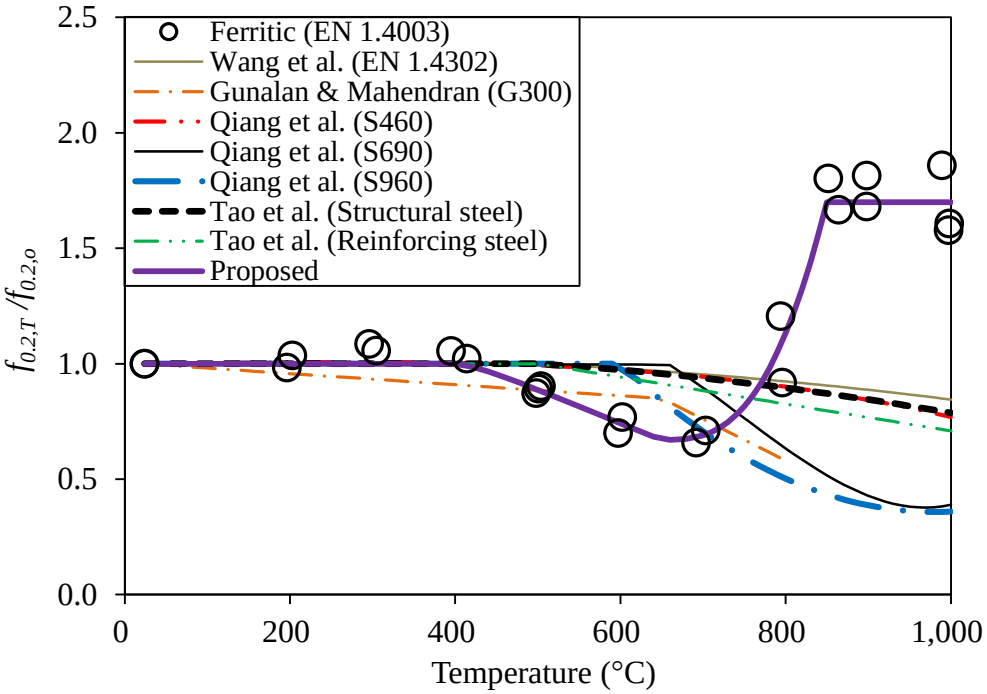

Fig. 9. Residual factor of yield strength.

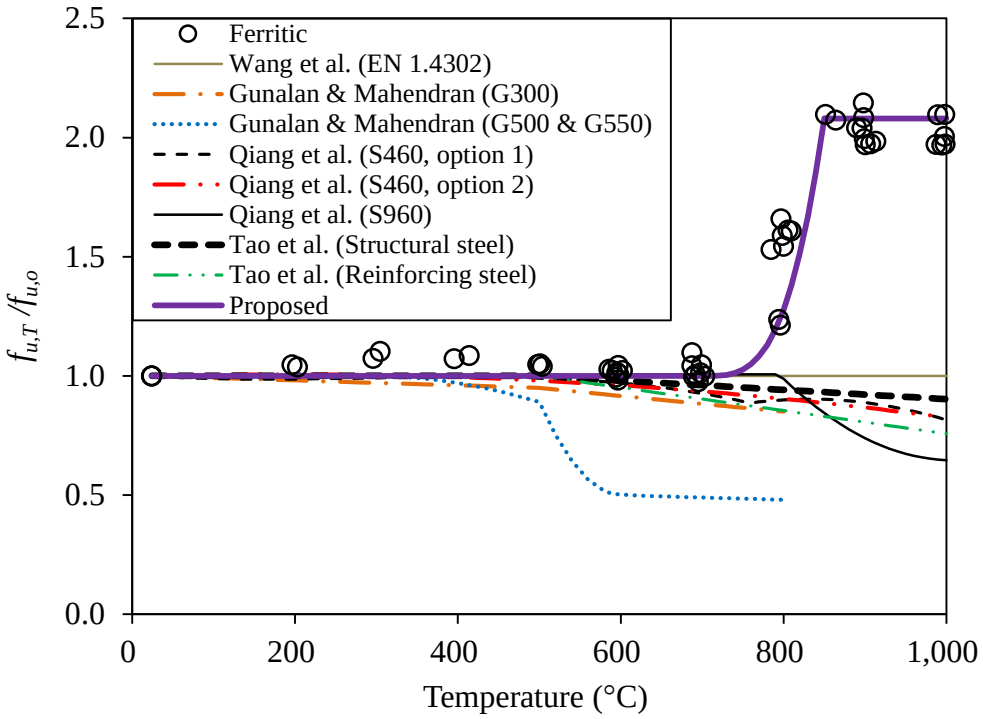

Fig. 10. Residual factor of ultimate strength.

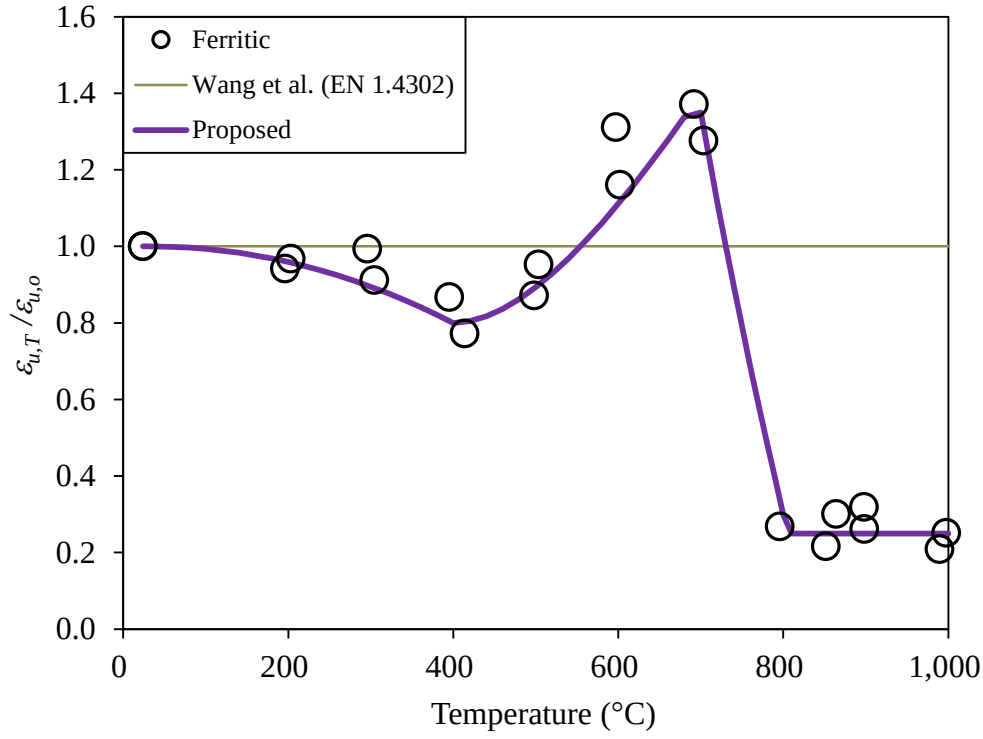

Fig. 11. Residual factor of strain at ultimate strength.

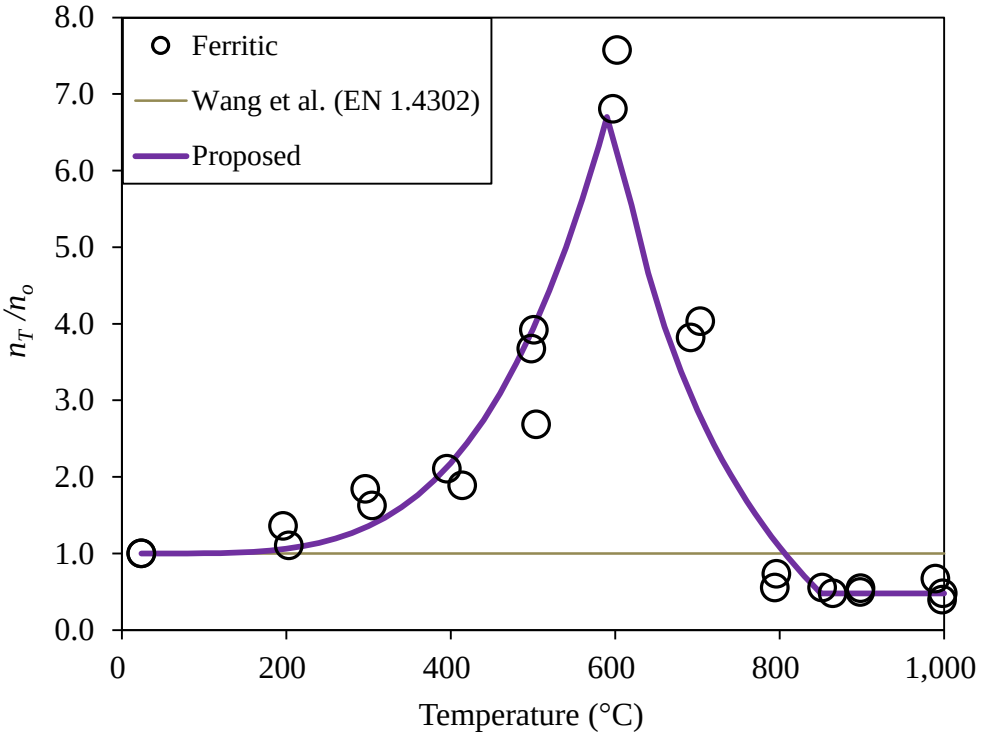

Fig. 12. Residual factor of Ramberg-Osgood parameter.

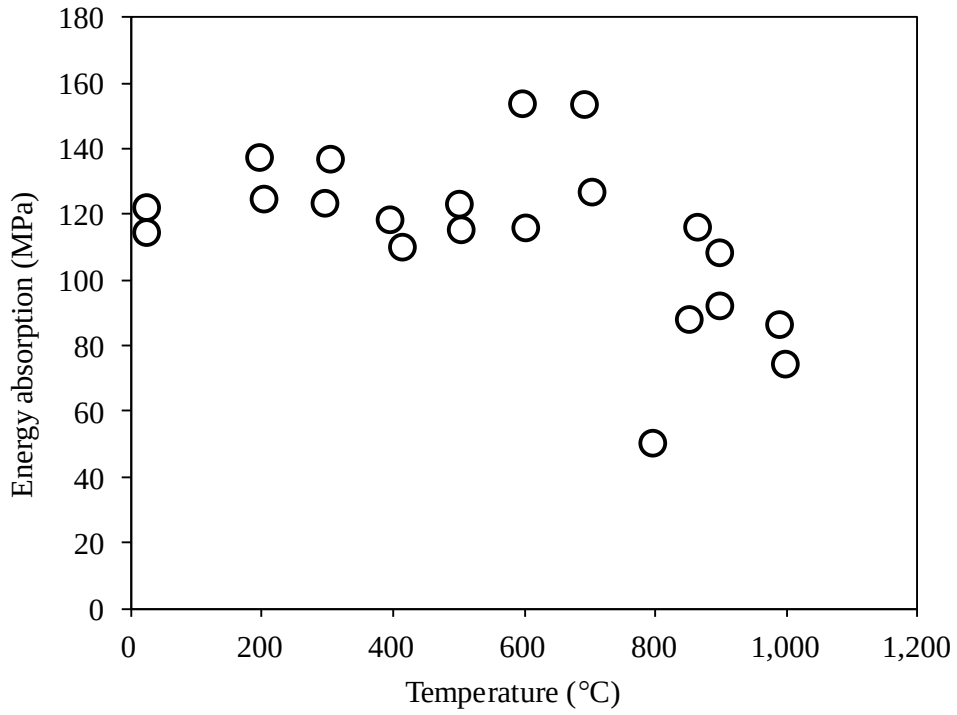

Fig. 13. Energy absorption of ferritic stainless steel at different temperatures.

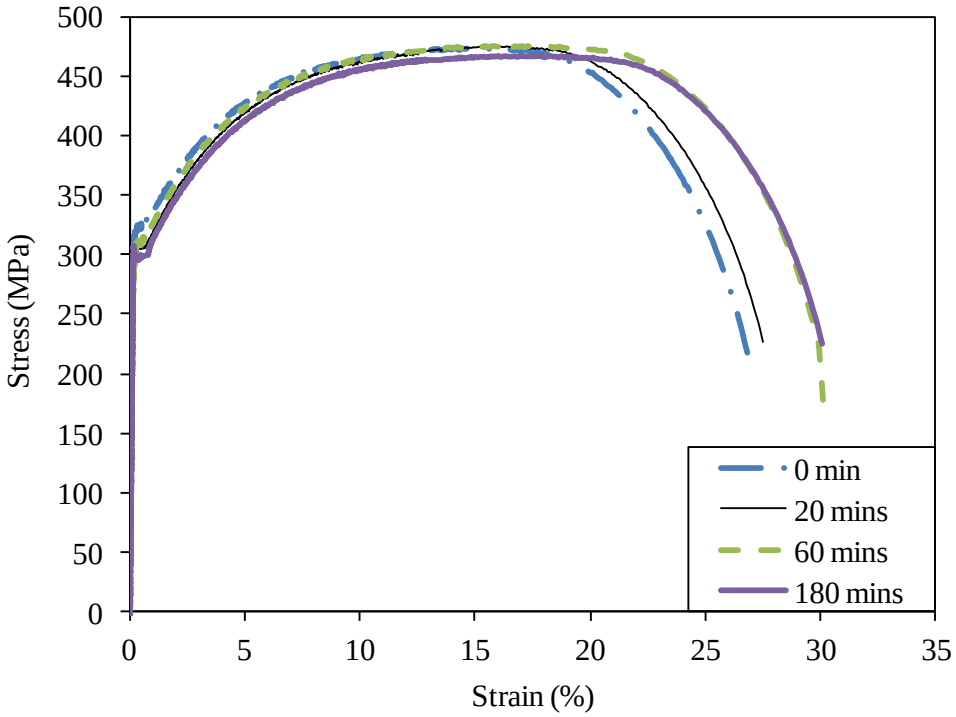

Fig. 14. Stress-strain curve of ferritic stainless steel at 600 °C with different soak time.

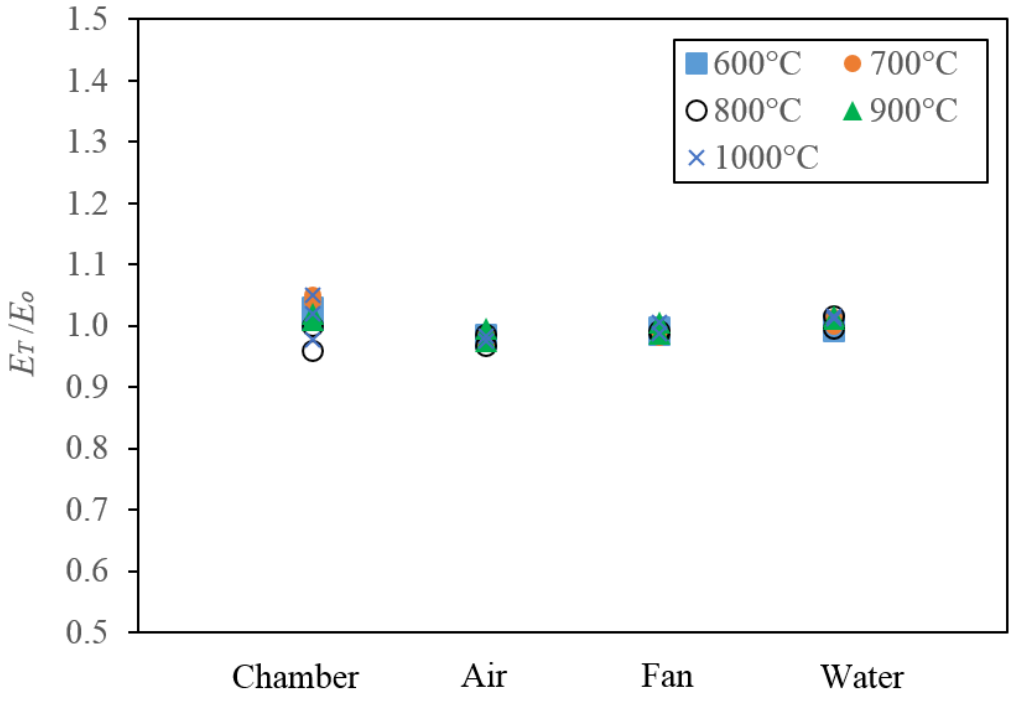

Fig. 15. Young's modulus for ferritic stainless steel with different cooling rates.

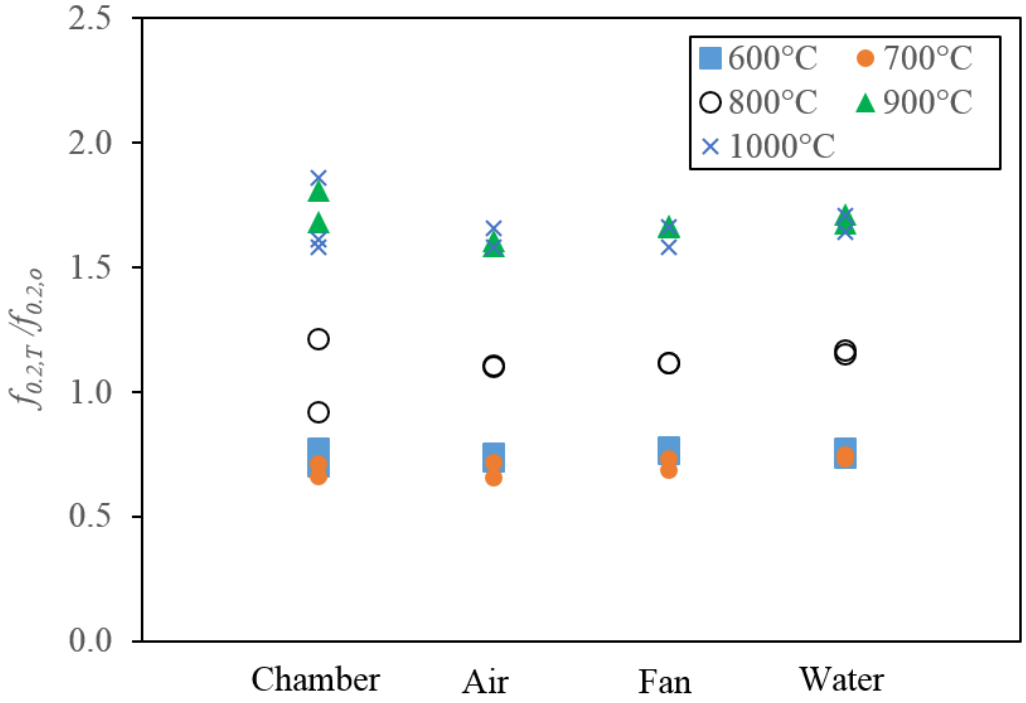

Fig. 16. Yield strength for ferritic stainless steel with different cooling rates.

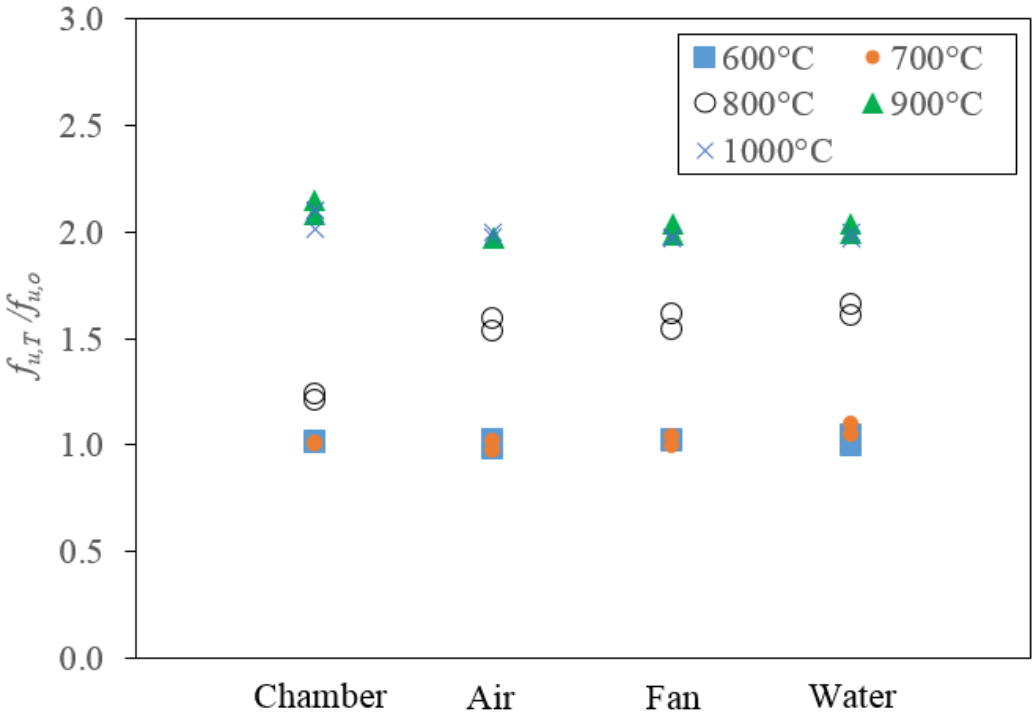

Fig. 17. Ultimate strength for ferritic stainless steel with different cooling rates.

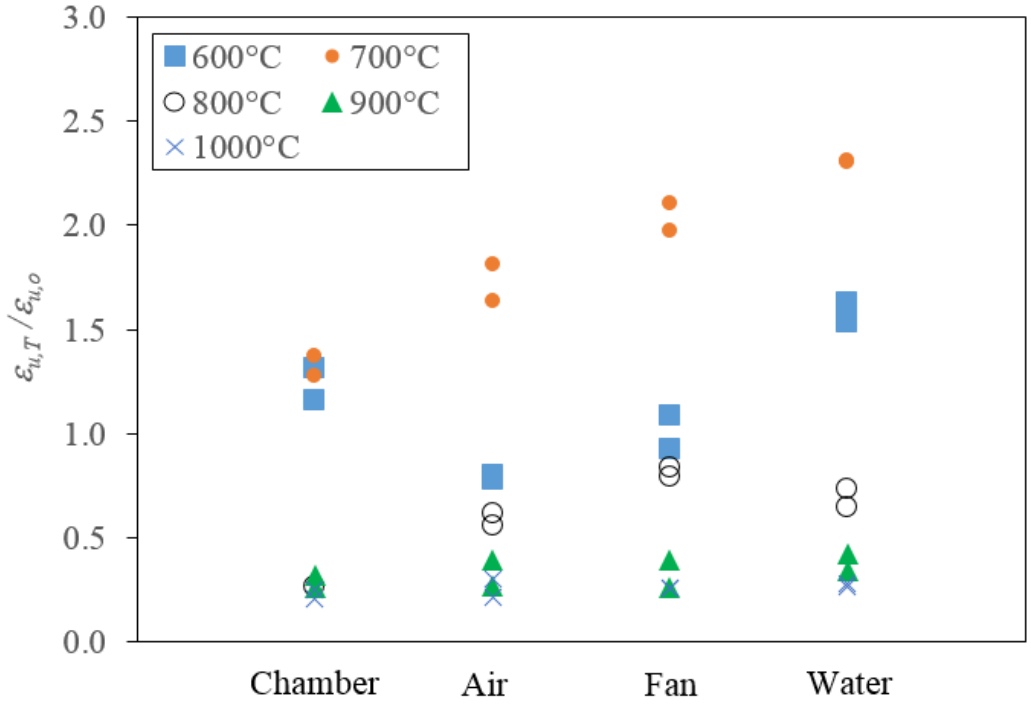

Fig. 18. Strain at ultimate strength for ferritic stainless steel with different cooling rates.

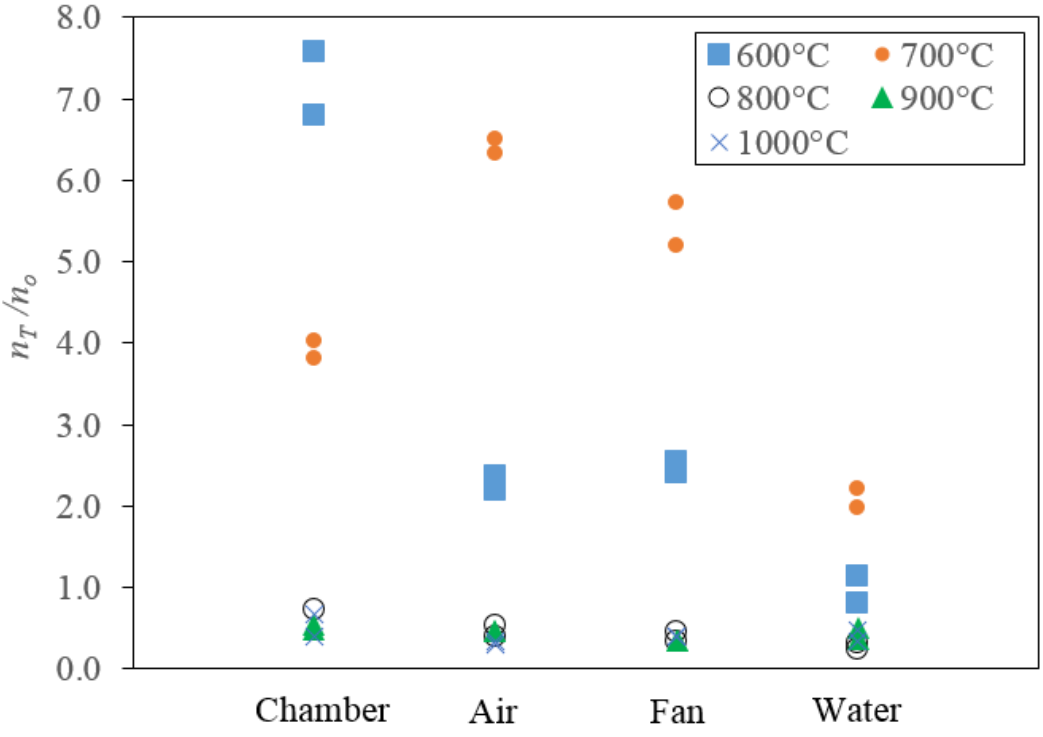

Fig. 19. Ramberg-Osgood parameter for ferritic stainless steel by different cooling rates.

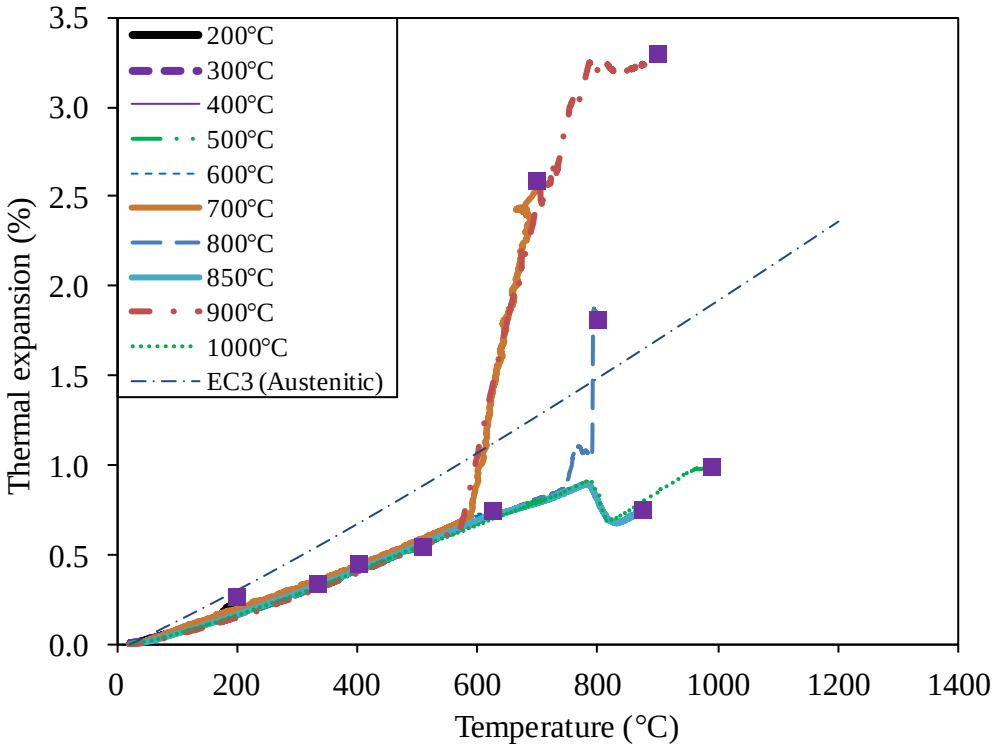

Fig. 20. Thermal elongation predicted by EC3 with ferritic stainless steel test results

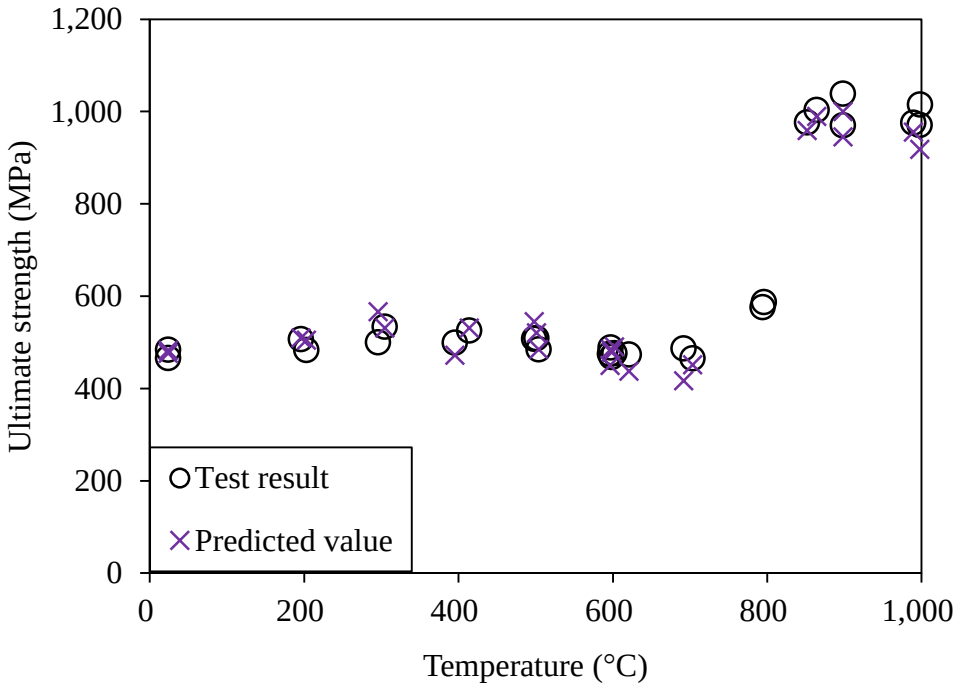

Fig. 21. Comparison of the test results and predicted value of ultimate strength for ferritic stainless steel.

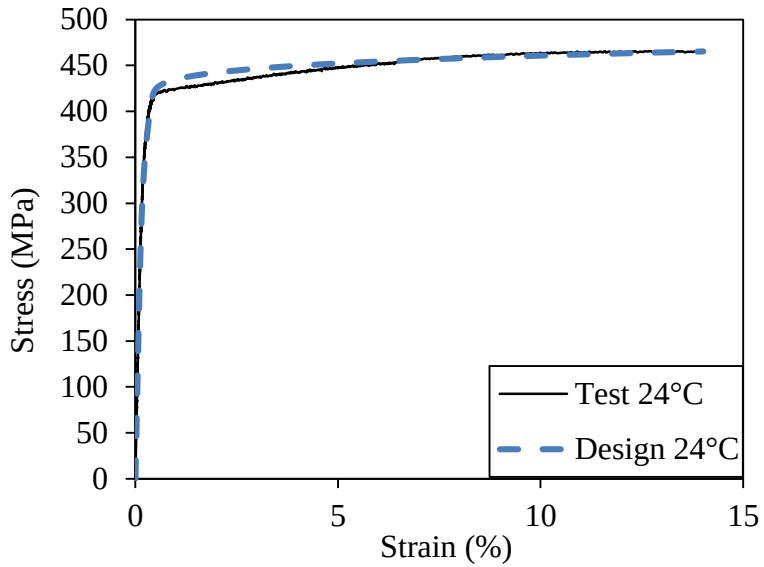
Stress (MPa)
Strain (%)
Test 24°C
Design 24°C

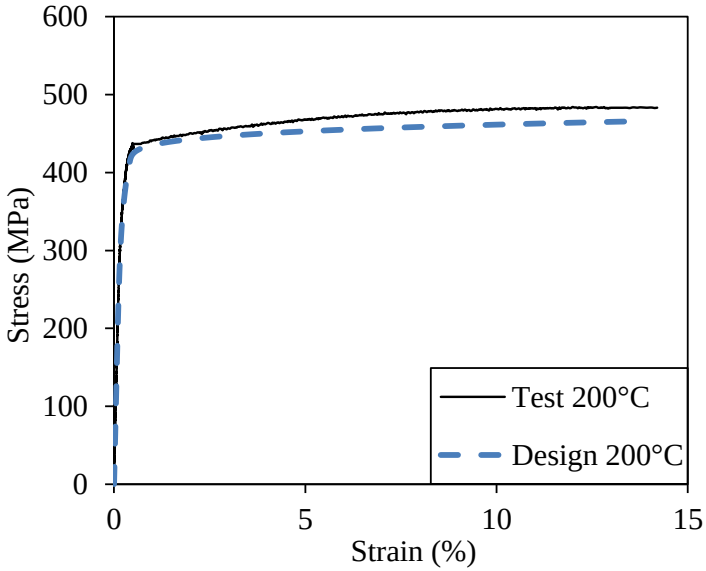
Stress (MPa)
Strain (%)
Test 200°C
Design 200°C

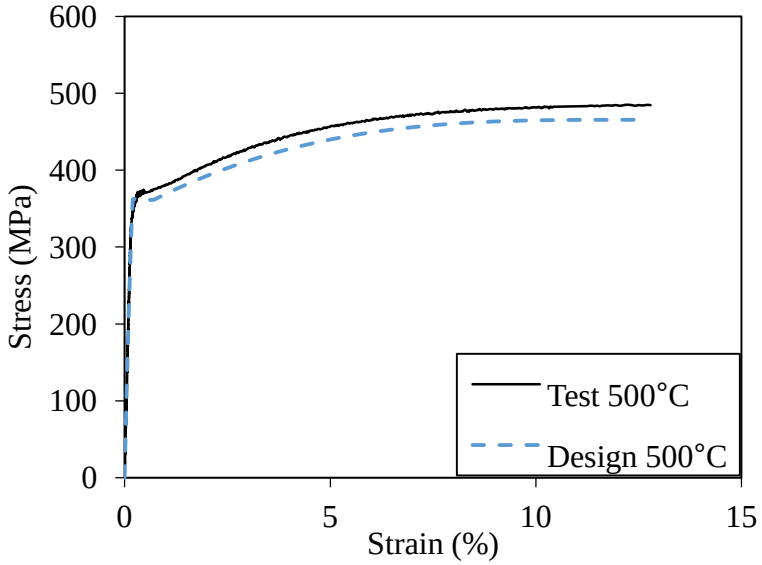
Stress (MPa)
Strain (%)
Test 500°C
Design 500°C

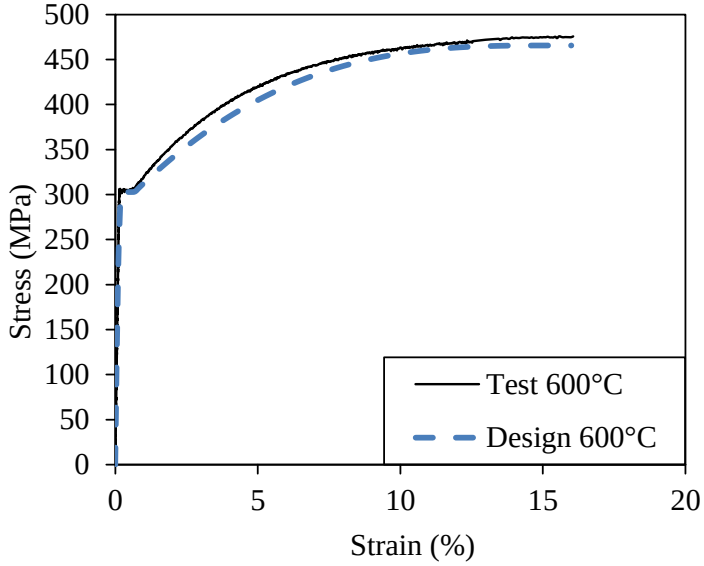
Stress (MPa)
Strain (%)
Test 600°C
Design 600°C

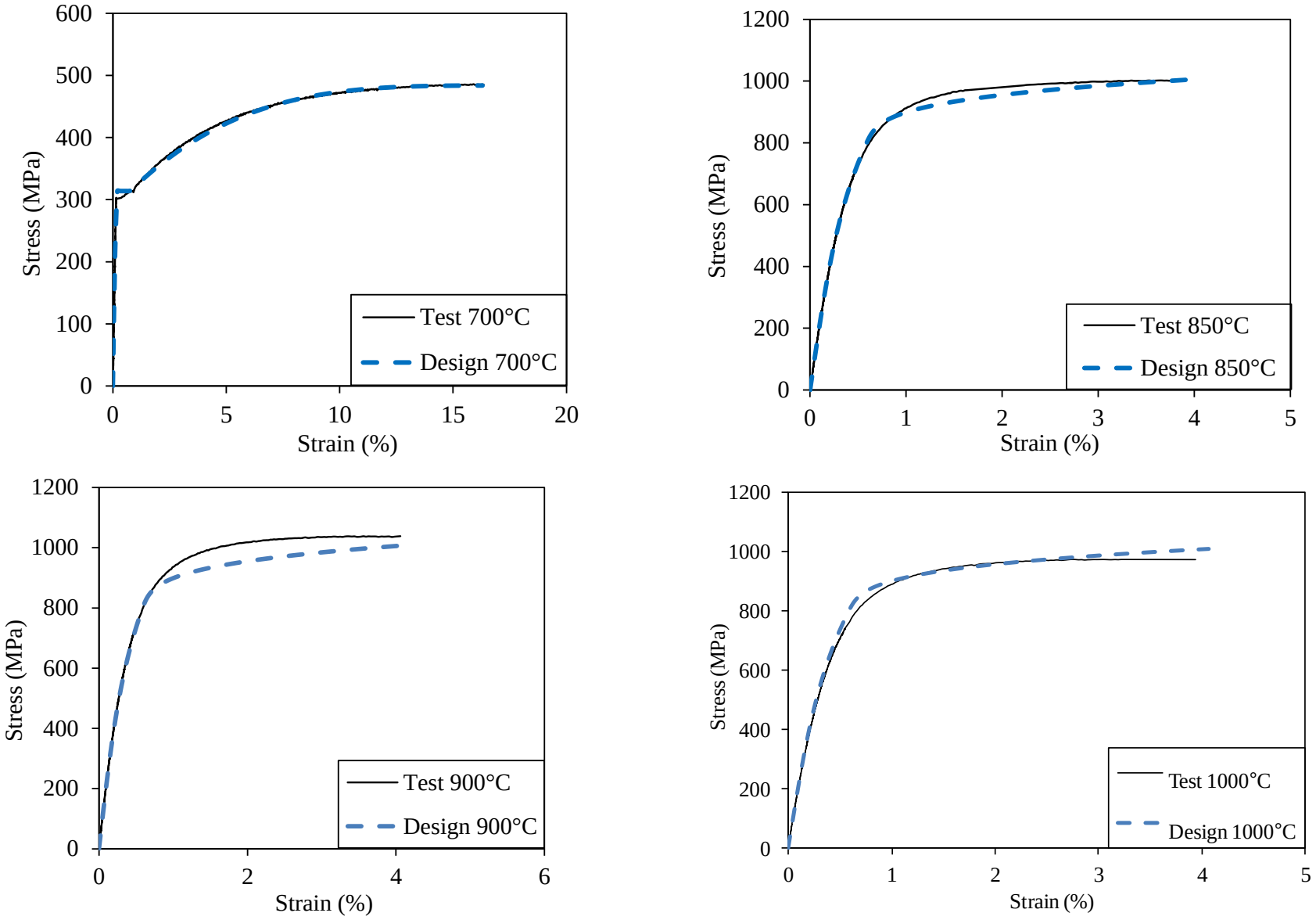

Fig. 22. Stress-strain curve of ferritic stainless steel (section 120×80×3)